Bioorthogonal tools to study fatty acid uptake in immune cells

Bertheussen, K.

3

Global Identification of Protein Oleoylation in Dendritic Cells by Pull-Down Chemical Proteomics

Abstract

Protein lipidation is a cellular process which increases protein diversity, and is important for correct protein function, signalling, transportation, and regulation. Protein lipidation has also been shown to be necessary for the correct functioning of the innate and adaptive immune responses. By incorporating a bioorthogonal modification in the fatty acyl chain of fatty acids, global protein lipidation patterns can be studied. In this Chapter, sterculic acid (StA) is used as a bioorthogonal probe to study protein oleoylation (the modification of proteins with oleic acid) in dendritic cell line DC2.4. A library of tetrazine-modified biotin molecules was synthesised and tested for their cell-permeability and reactivity with StA. Here, tetrazines **17** and **19** were identified as cell-permeable and were compared to biotin-PEG4-tetrazine in a pull-down chemical proteomics approach. Different proteins were identified as oleoylated with the three compounds. It is suggested that the physicochemical properties of the compounds, as well as spacer length between the tetrazine and biotin moieties, influence which proteins are detected. Several proteins with known immunological functions were found to be oleoylated, including proteins (e.g. SLC15A3) for which this modification had not previously been reported.

Parts of this chapter are adapted from the publication:

K. Bertheussen, M. van de Plassche, T. Bakkum, B. Gagestein, I. Ttofi, A. J. C. Sarris, H. S. Overkleeft, M. van der Stelt, S. I. van Kasteren, *Angew. Chem. Int. Ed.* **2022**, *61*.

Introduction

Homo sapiens has a surprisingly low number of open reading frames (ORFs) in its genome. However, these approximately 20,000 genes form the basis for over one million proteins.[1] Multiple processes exist that increase the diversity and complexity of the proteome, compared to the original genetic information. Alternative splicing is one of these mechanisms, where a single gene can give rise to multiple mRNA transcripts, and thereby also different proteins with distinct structures and functions.[1] Proteins can also undergo various chemical modifications, which – as the name would suggest – are modifications on the peptide structure that are introduced after translation. Many distinct post-translational modifications (PTMs) exist, among others acetylation, phosphorylation, ubiquitination, glycosylation, and lipidation, and they are all important for the correct folding, function, signalling, and transportation of the modified proteins.[2]

Proteins can be modified with a number of lipids, such as fatty acids (FAs)[3], cholesterols[4], isoprenoids (such as farnesyl or geranylgeranyl)[5], or glycosylphosphatidylinositol-anchors (GPI-anchors).[6] These lipid molecules are covalently linked to cysteine, lysine, threonine, or serine sidechains, or the C- or N-terminus of the protein, via thioester, amide, thioether, or ether linkages.[2,7] Protein lipidation is associated with increased hydrophobicity of the target protein, which can be essential for regulating protein configuration, trafficking, stability, and localisation. Due to their increased hydrophobicity, lipidated proteins are often associated with biological membranes, where the lipid tail is embedded in the lipid bilayer.[7]

Protein lipidation, and especially the reversible S-palmitoylation modification, has been implicated in several functions in both innate and adaptive immunity, where it is responsible for the clustering of various important immune molecules to cellular membranes.[8] In innate immunity it has been shown that S-palmitoylation is important for the correct function and localisation of important innate immune receptors such as Toll-like receptor 2 (TLR2)[9], and MyD88 (a signalling adapter protein for TLRs).[10] Stimulator of interferon genes (STING) is a signalling protein that is involved in the immune response to DNA in the cytosol. Upon activation, STING is also S-palmitoylated, which leads to the activation of nuclear factor-κB (NF-κB) and interferon regulator factor 3 (IRF3), which in turn results in the production of proinflammatory cytokines and type-I interferons.[11]

There are also several examples of the importance of S-palmitoylation in the T-cell receptor (TCR) signal transduction pathway of adaptive immunity.[12] It has been shown that TCR coreceptors CD4 and CD8 are S-palmitoylated, and that this is necessary for the correct clustering of the TCR complex and downstream signalling subunits (such as Src family protein tyrosine kinase Lck).[13–15] Lck itself can also be S-palmitoylated, a PTM that is required for its correct plasma membrane localisation, CD4 association, and downstream signalling.[16–18]

Although these examples emphasize the importance of S-palmitoylation as an immunomodulating regulator, a proteome-wide understanding of how protein lipidation affects immune cell function, and activation, is still lacking. There is also little information about other forms of protein lipidation, and how they affect immune cell function. To elucidate this intricate balance on a global level, appropriate

chemical tools are needed that allow the selective retrieval of the lipidated part of the proteome under different biological conditions.

Bioorthogonal, or click, chemistry could serve this purpose.[2] Most bioorthogonal modifications of lipids have been applied to the modification of lipid headgroups. This offers selectivity for which lipid class the analogue will be incorporated into. There have e.g. been reports of the phospholipid class phosphatidylcholine (PC) being labelled in this way.[19] *De novo* PC biosynthesis occurs via the Kennedy pathway, where an activated choline molecule is coupled to diacylglycerol to form PC. The alkyne- and azide-containing choline analogues propargylcholine[20] and azidocholine[21], respectively, have successfully and selectively been shown to label up to 50% of the cellular pool of PC (Figure 1A).

However, since lipids react with proteins via their hydrophilic head groups, a modification in that part of the molecule will result in an impaired ability to lipidate proteins. To this end, strategies where the bioorthogonal modifications are instead located in the fatty acyl chain have been developed.[2] Perhaps the most studied bioorthogonal variants of this sort, are lipids modified with an alkyne[9,22–29] or azide[30–34] moiety at the ω-position of the fatty acyl chain (Figure 1B). This ensures a more global labelling of cellular lipids such as triglycerides, phospholipids, and glycolipids. However, these modifications also allow the study of different forms of protein lipidation (e.g. palmitoylation, myristoylation, or prenylation).[2] This approach has aided in the discovery of many new palmitoylated proteins in mammalian cells[9,22,35,36], as well as implicating the relevance of certain palmitoylated proteins in diseases like cancer[37], and bacterial or viral infections.[38]

Far less is known about the more obscure PTM, protein oleoylation (the modification of proteins with oleic acid). This PTM has previously been studied with alkyne-modified oleic acid analogues[39], but although protein oleoylation has been shown to occur in multiple proteins[39–41], not much is known about this PTM on a proteome-wide level. In Chapter 2 of this thesis, it was described how the addition of sterculic acid (StA) to dendritic cell line DC2.4, and the subsequent labelling with tetrazine-fluorophore conjugates, led to a fluorescent signal visible throughout the entire cell. This led to the conclusion that cellular membranes (including organellar membranes) were labelled with StA. However, it also posed the question if proteins could be labelled with the oleic acid analogue, StA, as a PTM, and if this bioorthogonal oleic acid analogue could be used to study protein oleoylation by chemical proteomics in immune cells. In this Chapter, by applying a library of tetrazine-modified biotin molecules, it was found that proteins can indeed be modified with StA as a PTM. It was further shown that tetrazine-modified biotins with different physicochemical properties influenced which proteins were detected as oleoylated. In addition, the comparison of live-cell versus cell lysate labelling also yielded different protein oleoylation patterns. Interestingly, several of the detected proteins are known to have key immunological functions, for example, the important immunoregulatory channel protein SLC15A3 was found to be differentially oleylated in these experiments. SLC15A3 has never been shown to be lipidated before, and therefore a novel regulatory mechanism of this protein involving protein oleoylation, is proposed.

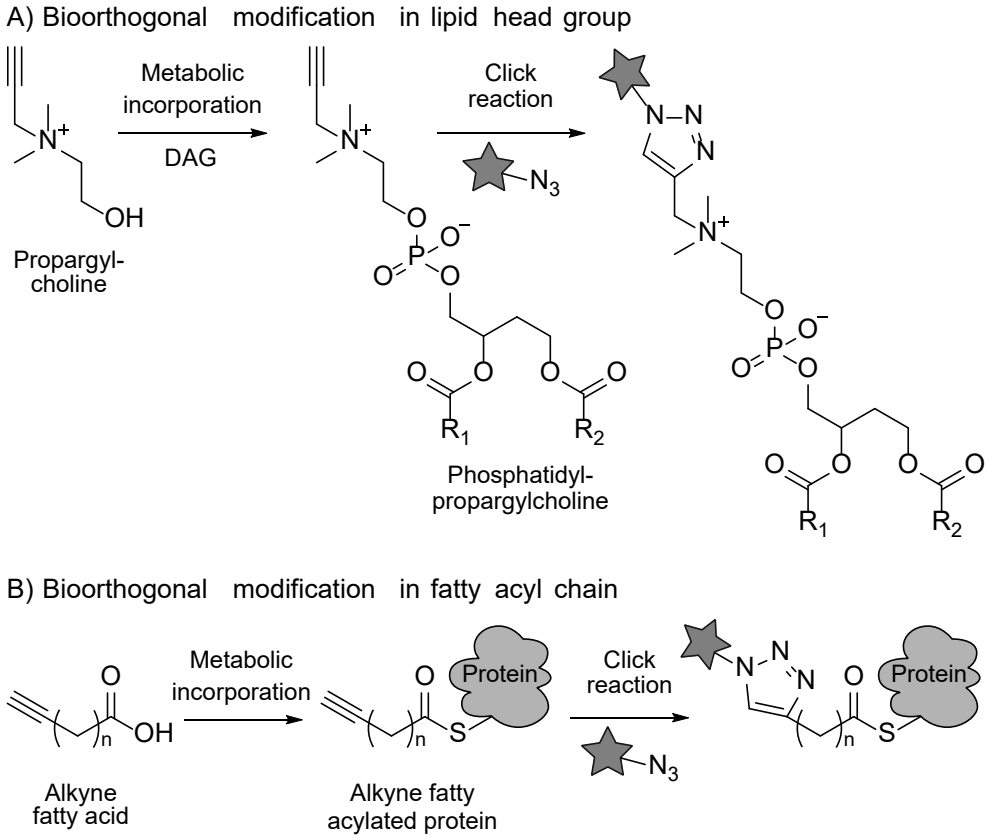

Figure 1: *Bioorthogonal modifications present in* ***A)*** *the lipid head group; allow for the metabolic incorporation of for example propargylcholine, which upon reaction with diacylglycerol (DAG) forms phosphatidylpropargylcholine, and subsequent labelling via a click reaction with an azide-tagged reporter group (star)[20], or* ***B)*** *the fatty acyl chain; allow for the metabolic incorporation of an alkyne-tagged fatty acid into a fatty acylated protein, and subsequent labelling via a click reaction with an azide-tagged reporter group (star).[9,22–29]*

Results & Discussion

Proteins can be modified with sterculic acid at a post-translational level

Here, it was first explored whether proteins can be covalently modified with StA as a PTM. DC2.4 cells were incubated with StA followed by cell lysis and click reaction with the cell-impermeable tetrazine-modified fluorophore **3** (Figure S1A, see Chapter 2). The proteins were resolved by SDS-PAGE, and the gel was fluorescently imaged (Figure 2A). However, since lipidated proteins are inherently more hydrophobic[42], and the lipid tail often resides in biological membranes[43], a live-cell click approach with the cell-permeable quenched tetrazine-modified fluorophore **7** (Figure S1B, see

Chapter 2) was also performed. In this approach, the hydrophobic fluorophore **7** could pass through cell membranes and react with the lipid in its naturally occurring location, whereafter the cells were lysed, and the proteins were resolved by SDS-PAGE (Figure 2B). In both cases fluorescent protein bands were visible. This indicates that a number of proteins were covalently modified with StA. Comparing the two approaches, it was clear that which proteins were labelled, differed under the different labelling conditions (lysate or on live cells), as indicated by the distinct labelling patterns. Upon LPS stimulation, the lipidation patterns appeared to become brighter compared to lipidation of non-stimulated DCs (Figure 2). This could indicate that protein lipidation is increased upon DC maturation but could also be caused by an increased uptake of StA by the mature DCs and subsequently more labelling of proteins by this FA analogue compared to native FAs.

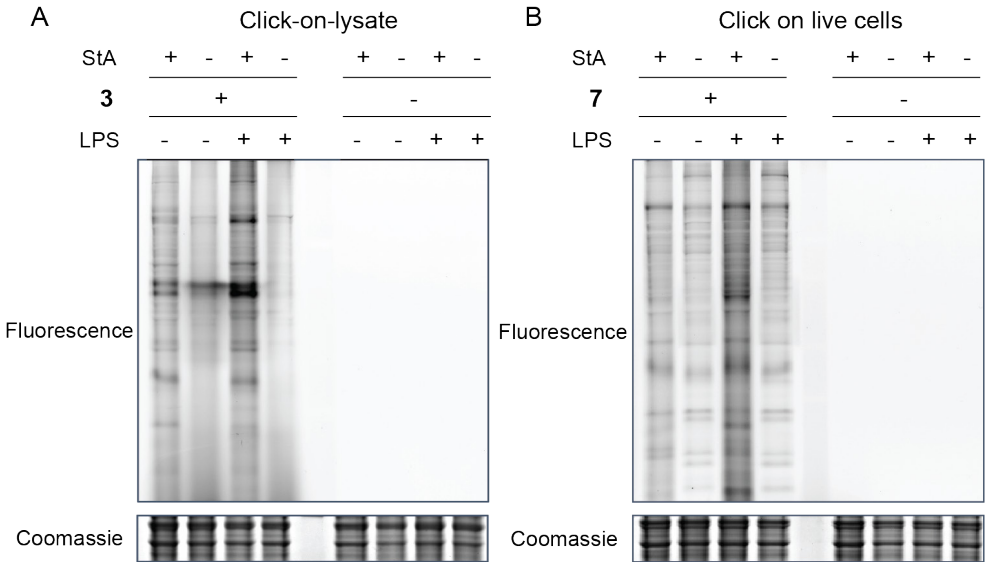

Figure 2: *Proteins can be modified with sterculic acid (StA) as a post-translational modification. DC2.4 cells were immature or matured with LPS (100 ng/mL) for 24 h and treated with StA (100 µM) for 20 h.* ***A)*** *The cells were harvested and lysed before IEDDA reaction with tetrazine-modified fluorophore* ***3*** *(10 µM) or vehicle for 2 h at RT.* ***B)*** *Live cells were subjected to IEDDA reaction with tetrazine-modified fluorophore* ***7*** *(10 µM) for 2 h at 37°C, before being harvested and lysed. All lysates were resolved on SDS-PAGE (12.5% acrylamide gels) and were measured for in-gel fluorescence. Coomassie staining served as a protein loading control.*

Chemical synthesis of library of tetrazine-modified biotin molecules

To further investigate these observed differences in lipidation pattern, a pull-down chemical proteomics approach was developed (Figure 3). A set of tetrazine-modified biotin molecules were designed and synthesised (as described below), which could be applied for the click reaction with StA. After StA uptake in DC2.4 cells (Figure 3A), the different tetrazine-modified biotins were added to the samples at different points in the protocol, either to the live cells or to the cell lysate (Figure 3B). The tetrazine

moiety could react with StA, whereas the biotin moiety allowed for pull-down of the lipidated proteins with streptavidin beads, followed by on-bead trypsin digestion and identification of the peptides by LC-MS/MS (Figure 3C). Thereby proteins that were modified with StA as a PTM could be quantitatively identified.

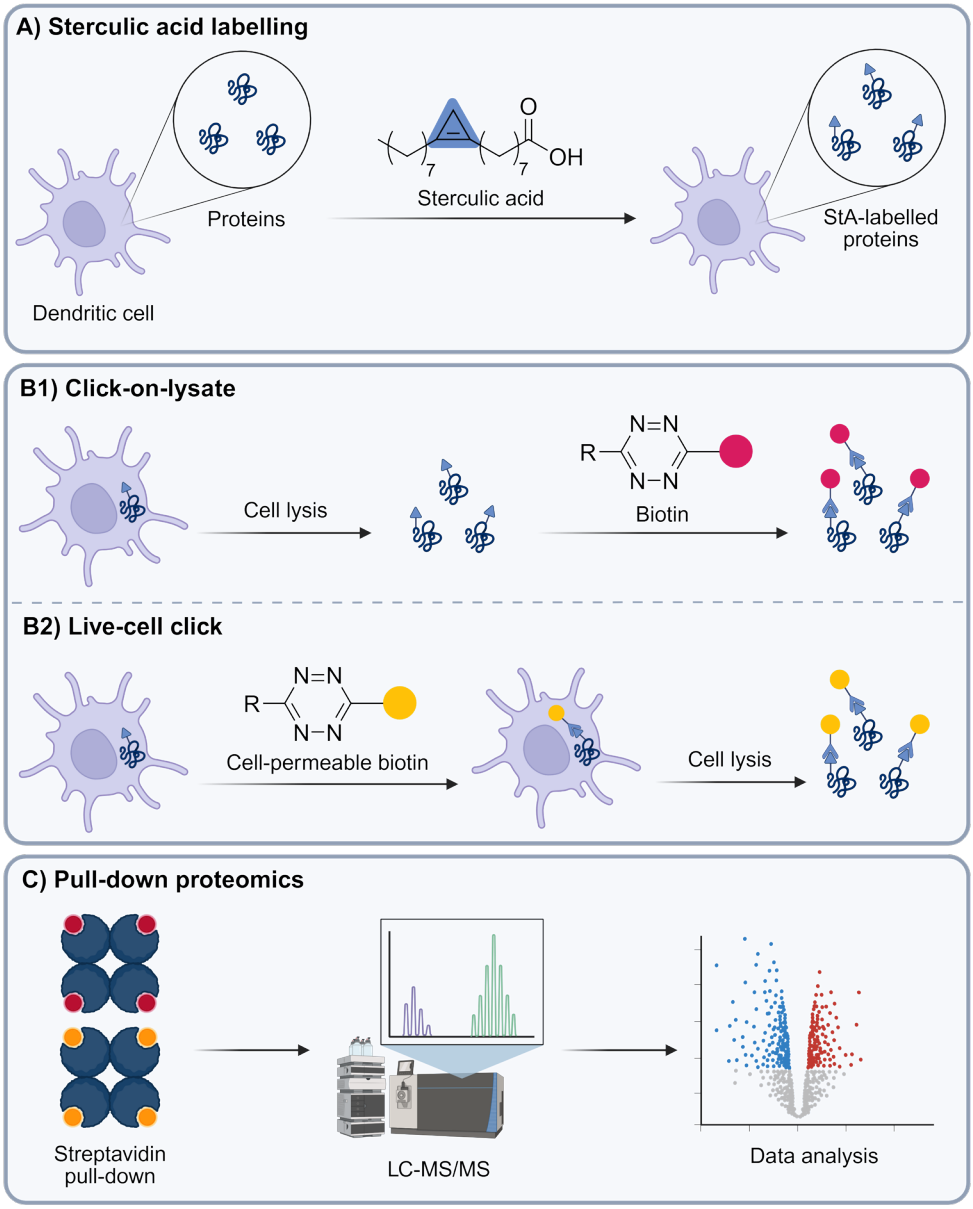

Figure 3: *Illustration of the pull-down proteomics approach to study protein lipidation with sterculic acid (StA) in a dendritic cell line (DC2.4). The approach consists of* ***A)*** *StA labelling of proteins, followed by* ***B)*** *click reaction with tetrazine-modified biotins in lysate (1) or on live cells (2), and* ***C)*** *pull-down proteomics. The figure is made with BioRender.*

To this end, several hydrophobic tetrazine-modified biotins (**16**-**21** and **29**-**31**) were synthesised (Scheme 1) and compared to the hydrophilic biotin-PEG4-tetrazine (Figure S1C) for their cell permeability under live cell conditions. For **16**-**21** and **29**-**31**, two different spacer lengths were chosen between the tetrazine and biotin moieties. One contains only the valeric acid moiety of biotin and is a short spacer (Biotin, Scheme 1). The other spacer contains an additional lysine group and is a medium length (LC-Biotin, Scheme 1). The synthesis of **16**-**21** (Scheme 1A) was based on the synthesis of previously published BODIPY-FL tetrazine conjugates.[44,45] Instead of the BODIPY fluorophores, a biotin moiety was coupled to the amine function of the tetrazines.

The synthetic route started from 4-(aminomethyl) benzonitrile of which the free amine was protected with a *tert*-butyloxycarbonyl (Boc) group using di-*tert*-butyl dicarbonate and DIPEA, yielding compound **9**. This compound was converted into *N*-Boc-protected aminoalkyl-tetrazines **10**-**12** by a Lewis acid-catalysed condensation of the nitrile with hydrazine, followed by oxidation with sodium nitrite under acidic conditions.[46] The protected amine of tetrazines **10**-**12** was deprotected using HCl/dioxane, and tetrazines **13**-**15** were immediately coupled to either the commercially available biotin or LC-biotin via an NHS coupling, resulting in tetrazine-modified biotins **16**-**21**. These compounds were all poorly soluble in DMSO, with solubility decreasing with increasing spacer length (**19**-**21**). Compounds **16**-**21** were attempted dissolved at 30 mM (in DMSO), but only **16**-**18** were soluble at this concentration. Compounds **19**-**21** were first soluble in DMSO at 10 mM concentrations.

To improve the solubility of these compounds, another set of tetrazine-modified biotins (**29**-**31**) were designed and synthesised (Scheme 1B). These compounds lacked the benzylic ring of **16**-**21** in an attempt to increase their solubility, while still retaining their cell-permeability. This synthetic route started with the Boc-protection of 3-aminopropionitrile to form **22**. Thereafter, similarly to the previous synthesis, the conversion into *N*-Boc-protected aminoalkyl-tetrazines **23**-**25**, followed by deprotection into tetrazines **26**-**28**, was performed. Lastly, an NHS coupling to biotin resulted in the tetrazine-modified biotins **29**-**31**. As expected, the solubility of these compounds had improved compared to that of **16**-**21**.

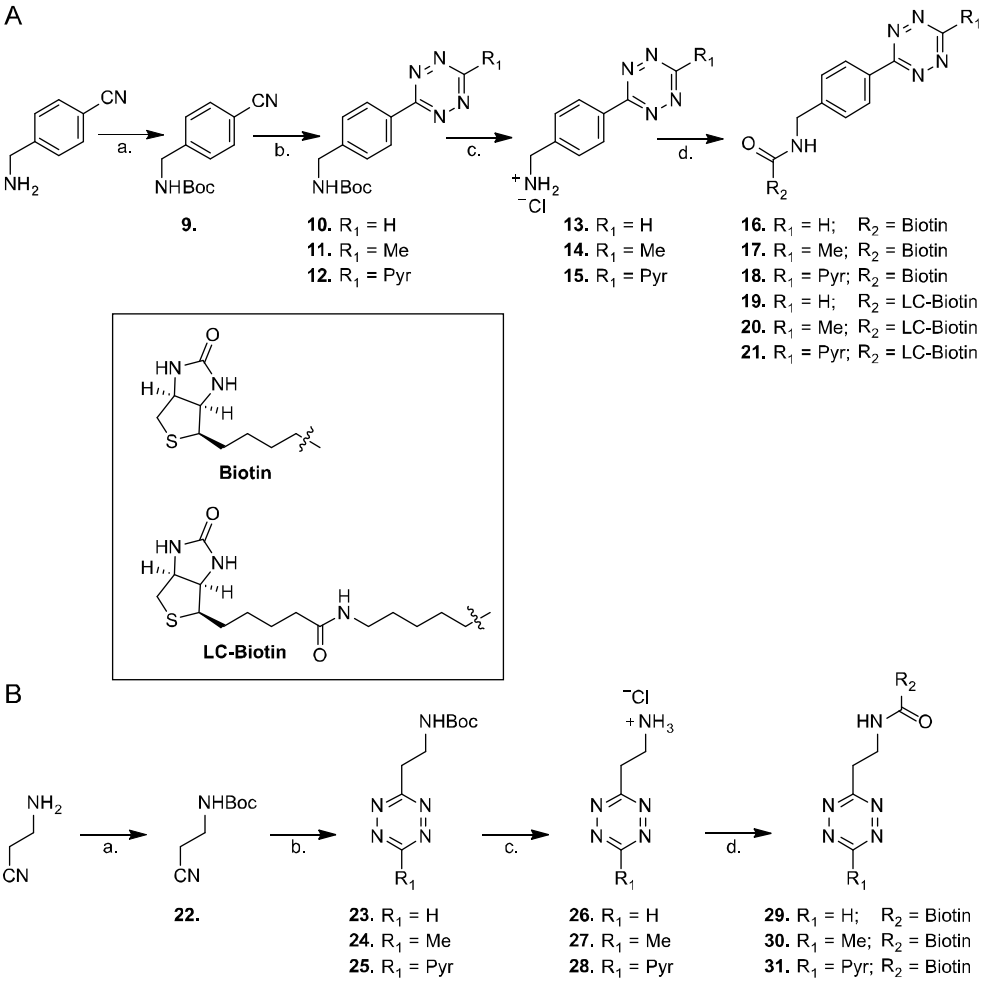

Scheme 1: *The synthesis of hydrophobic tetrazine-modified biotins* ***16-21*** *and* ***29-31****.* ***A)*** *a) Boc_2O, NaOH, H_2O, quant.; b) I) hydrazine monohydrate, $Zn(OTf)_2$, formamidine acetate/ acetonitrile/2-cyanopyridine, 60-80°C; II) $NaNO_2$, AcOH/DCM (1:1, v:v), 9-33% over two steps; c) 4 M HCl in dioxane, anhydrous DCM, 90-100%.; d) NHS-biotin/NHS-LC-biotin, DIPEA, DCM, 40-73%.* ***B)*** *a) Boc_2O, anhydrous DCM, 98%; b) I) hydrazine monohydrate, $Zn(OTf)_2$/ $Ni(OTf)_2$, formamidine acetate/acetonitrile/2-cyanopyridine, 20-60°C; II) $NaNO_2$, AcOH/DCM (1:1, v:v) or 4 M $NaNO_2$, 2 M HCl, 2-22%; c) 4 M HCl in dioxane, anhydrous DCM, 93-100%; d) NHS-biotin, DIPEA, DCM, 38%-73%.*

Testing permeability and reactivity of tetrazine-modified biotin library

To verify if the tetrazine-modified biotins were cell-permeable and could react with StA, live DC2.4 cells preloaded with StA were reacted with **16**-**21**, **29**-**31**, or biotin-PEG4-tetrazine. After the click reaction, any unreacted compound was washed away, and the cells were fixed and permeabilised. The addition of a streptavidin AZDye 647 conjugate was used to fluorescently label the biotin molecules that had entered the cells and reacted with StA. Lastly, the cells were imaged by fluorescence widefield microscopy (Figures 4 & S2).

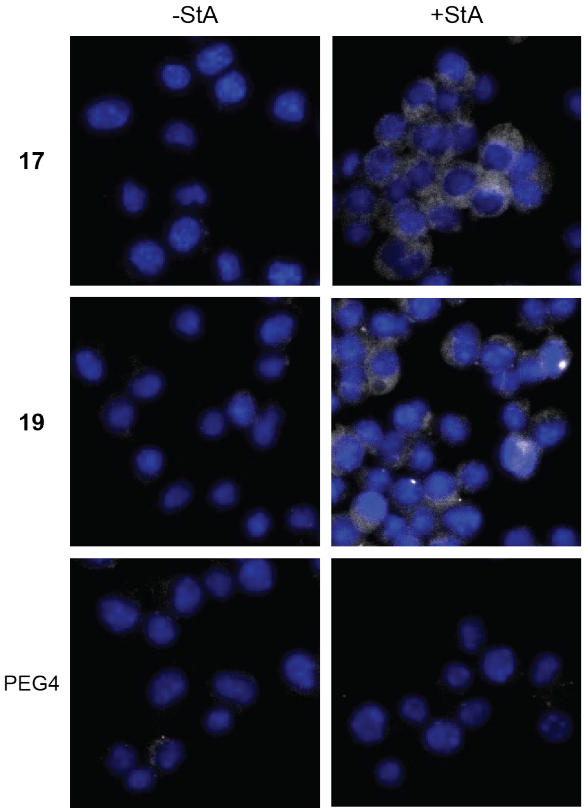

Figure 4: *Fluorescent microscopy verifies that compounds **17** and **19** are cell-permeable and reactive with StA. Biotin-PEG4-tetrazine (PEG4) is used as a negative control. To allow uptake of the fatty acid, DC2.4 cells were incubated with sterculic acid (+StA, 100 μM) or vehicle control (-StA) for 1 h. The respective tetrazine-modified biotins (200 μM) were then added and incubated for 4 h, before unreacted compound was washed away. The cells were fixed and permeabilised, and a streptavidin AZDye 647 conjugate (grey) was added to visualise the location of the reacted biotins. The nuclei were counterstained with Hoechst 33342 (blue) for reference.*

Compounds **17** and **19** showed detectable labelling over background, indicating that these two compounds are cell-permeable and able to react with StA. As expected, biotin-PEG4-tetrazine showed no signal in live cells, likely due to its hydrophilic PEG-spacer making it cell-impermeable (Figure 4). The rest of the compounds did

not show detectable labelling over background in live cells (Figure S2), indicating that these compounds are either cell-impermeable, or unable to react with StA.

The click reaction with the tetrazine-modified biotins **16**-**21** and **29**-**31** was also performed on fixed and permeabilised cells. The rationale was that the cell permeation with detergent after fixation would negate any cell-permeability factors for the probes. Therefore, a fluorescent signal would be expected from all compounds that can react with StA (Figure S3). Compounds **17** and **19**, as well as biotin-PEG4-tetrazine, showed detectable labelling over background. In addition, **29** and **30** showed labelling in the StA sample, indicating that they are StA reactive. Control samples showed no labelling of StA in live and fixed cells if the tetrazine-modified biotins were not present (Figures S4 & S5), as well as if the compounds were added and immediately washed away (Figures S6 & S7). This indicates that true signal-over-background was observed in Figures 4, S2, and S3. Based on these results, compounds **17** and **19** were credited with sufficient cell-permeability and StA reactivity qualities for further proteomic analysis.

Identification of oleoylated proteins with mass spectrometry

Compounds **17** and **19** were selected for the live-cell approach of pull-down chemical proteomics (outlined in Figure 3). However, due to the precious nature of these compounds, the mass spectrometry methodology was first optimised on lysates with biotin-PEG4-tetrazine. To this end, LPS-matured or untreated immature DC2.4 cells were incubated with StA to allow for its incorporation as a PTM. After cell lysis, the click reaction with biotin-PEG4-tetrazine was performed, and the modified proteins could be isolated with streptavidin beads. After on-bead enzymatic digestion, peptides from the lipidated proteins were detected by mass spectrometry and analysed. When biotin-PEG4-tetrazine was applied in this click-on-lysate approach in immature DC2.4 cells, 242 proteins were identified as significantly enriched with StA (Figure 5A), compared to control. For mature DC2.4 cells that were stimulated with LPS, 246 significantly enriched proteins were detected over control (Figure 5B). The UniProt protein database categorises protein entries into specific subsets based on for example biological function or cellular localisation.[47] As annotated by UniProt keyword KW-0472 77 (32%) and 83 (34%), respectively, of the identified proteins are known to be membrane proteins.

When comparing the StA-enriched proteins between LPS-treated mature and untreated immature DCs, 3 proteins were significantly enriched in the mature DC samples, and 2 proteins in the immature sample (Figure 5C). It is not clear whether these proteins are detected due to changes in their expression levels, increased protein lipidation, or a combination of these two factors. However, of the upregulated proteins, two (CD14[48,49], SLC15A3[50–52]) are known to be upregulated upon LPS stimulation, but nothing has been reported on their change in lipidation status. The downregulated protein TMEM176B, has also previously been shown to be downregulated in DCs upon LPS stimulation.[53,54] These results validate the described method as a robust way to study protein lipidation as a PTM, and again indicates that StA can be incorporated as a PTM in proteins.

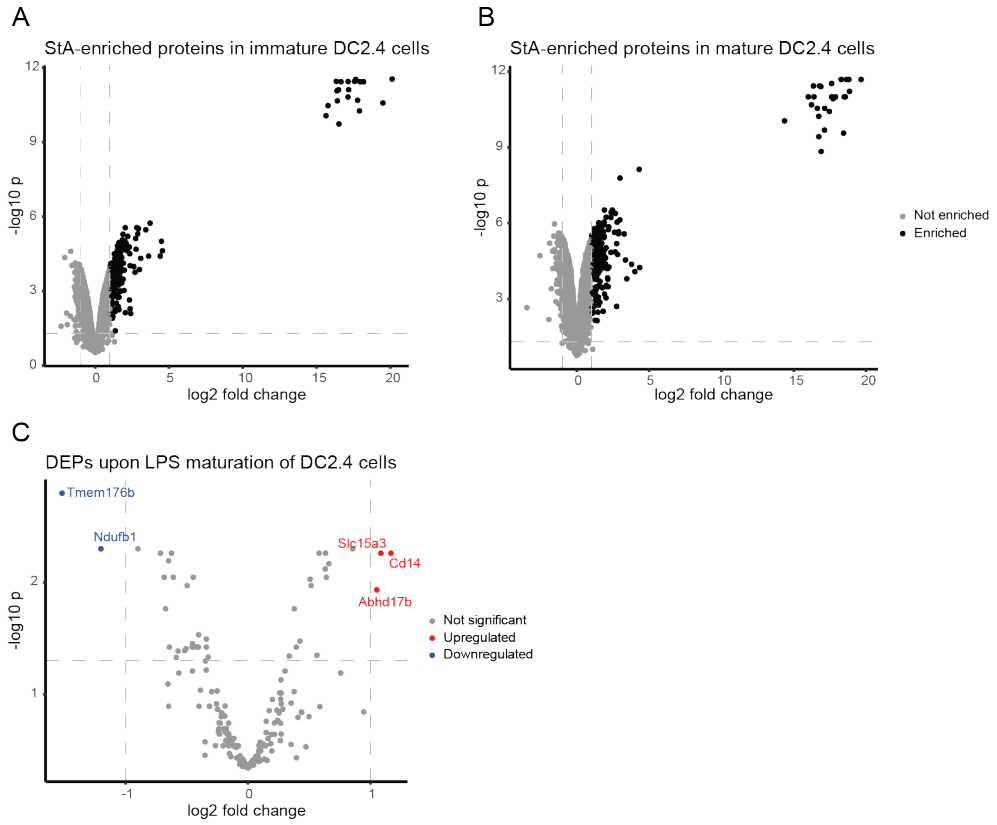

Figure 5: *Proteomic analysis of proteins modified with sterculic acid (StA) in DC2.4 cells by chemical proteomics. DC2.4 cells were immature or matured with LPS (100 ng/mL) for 24 h and treated with StA (10 µM) for 20 h. The cells were harvested and lysed, before IEDDA reaction with biotin-PEG4-tetrazine (200 µM) on the lysate. Shown are volcano plots of proteins identified in pull-down experiments in* ***A)*** *immature DC2.4 cells.* ***B)*** *LPS-matured DC2.4 cells. Proteins with a fold change >2 and p-value <0.05 are considered specifically enriched and are highlighted in black.* ***C)*** *Differentially StA-expressed proteins (DEPs) between mature and immature DC2.4 cells. LFQ-values of StA-enriched proteins were compared and proteins with significantly higher or lower LFQ abundance between the two conditions are marked in red and blue, respectively.*

Next, the pulldown protocol was applied to live cell labelling. Mature and immature DCs were labelled with StA for 20 hours at 10 µM, prior to the addition of **17** and **19**, followed by lysis, streptavidin-mediated retrieval, and mass spectrometry. For compound **17**, only 6 proteins were found to be StA-enriched in immature DCs (Figure 6A) and 10 proteins were found to be StA-enriched in mature DCs (Figure 6B). Of the enriched proteins, 2 (33%) and 2 (20%) proteins, respectively, were known membrane proteins (as annotated by UniProt keyword KW-0472[47]). Surprisingly, a completely different set of proteins than with the click-on-lysate approach with biotin-PEG4-tetrazine was retrieved for compound **17** in both mature and immature DCs (Table S1 & Figure S8).

For compound **19**, 11 proteins were found to be StA-enriched in immature DCs (Figure 6C) and 17 proteins were found to be StA-enriched in mature DCs (Figure 6D). Of the enriched proteins, 8 (73%) and 13 (76%) proteins, respectively, are known to be membrane proteins (as annotated by UniProt keyword KW-0472[47]). Only two proteins that were found to be significantly StA-enriched with **19** in immature DCs, were also detected with biotin-PEG4-tetrazine, whereas three common proteins were found in mature DCs (Table S1 & Figure S8).

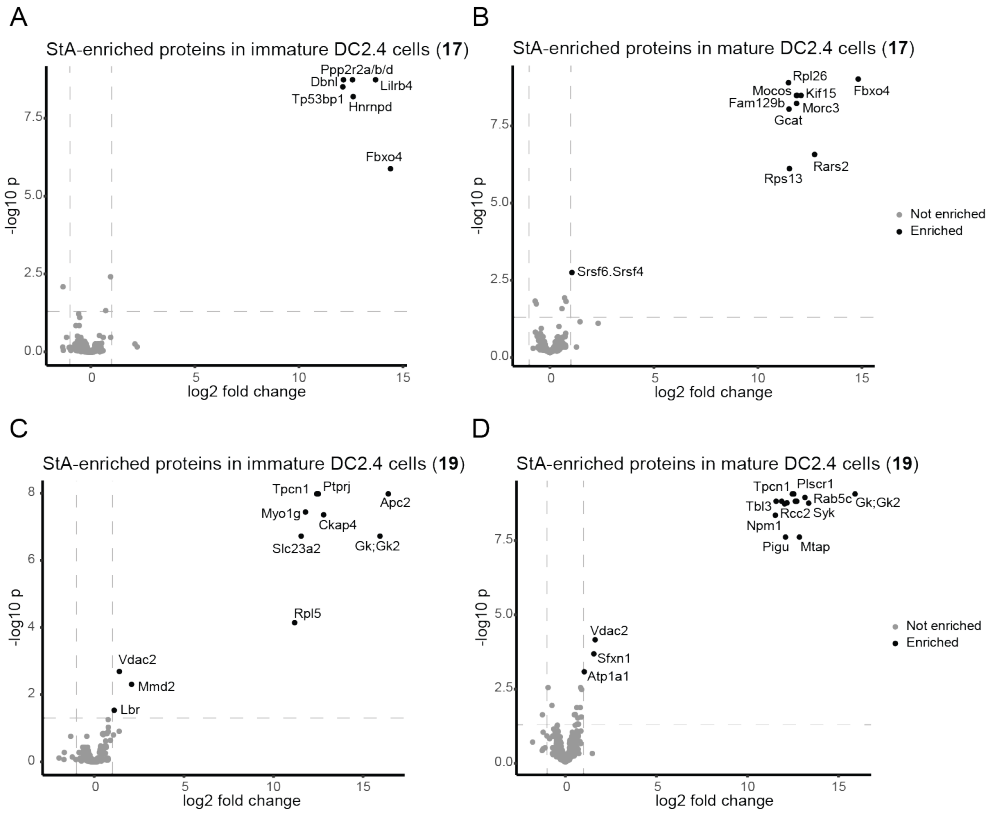

Figure 6: *Proteomic analysis of proteins modified with sterculic acid (StA) in DC2.4 cells by chemical proteomics. DC2.4 cells were immature or matured with LPS (100 ng/mL) for 24 h and treated with StA (10 μM) for 20 h. IEDDA reaction with* ***17*** *or* ***19*** *(200 μM) was performed on live cells, before the cells were harvested and lysed. Shown are volcano plots of proteins identified in pull-down experiments in* ***A)*** *immature DC2.4 cells with compound* ***17****.* ***B)*** *LPS-matured DC2.4 cells with compound* ***17****.* ***C)*** *immature DC2.4 cells with compound* ***19****.* ***D)*** *LPS-matured DC2.4 cells with compound* ***19****. All proteins with a fold change >2 and p-value <0.05 are considered specifically enriched and are highlighted in black.*

The lower numbers of StA-enriched proteins that were detected with the live-cell approach compared to the click-on-lysate approach could be caused by the need for **17** and **19** to diffuse through intact cells before encountering StA-lipidated proteins. It could also be affected by the hydrophobicity and poor solubility of the cell-permeable compounds **17** and **19**, causing them to be sticky. This could lead to more unspecific binding events, and thereby more noise in the MS data. In addition, the spacer

lengths between the biotin and tetrazine moieties in **17** (~13 Å) and **19** (~22 Å) are considerably shorter than the PEG4 spacer (~29 Å) of biotin-PEG4-tetrazine. These shorter spacers could lead to steric hindrance when the biotin-labelled proteins bind to the tetrameric streptavidin beads, impacting the number of proteins that can be pulled out. However, since the longer spacer in **19** also led to poorer solubility of the compound, further research is needed to fine-tune this relationship between solubility, cell-permeability, and spacer length.

The low amount of overlap between proteins detected with compound **19** and biotin-PEG4-tetrazine could indicate that tetrazine-modified biotins with different physicochemical properties might be preferential for certain proteins. As annotated by UniProt keyword KW-0472[47], ~75% of the proteins that were found to be StA-enriched with **19**, are known to be bound to or associated with membranes. For biotin-PEG4-tetrazine only ~30-35% of the StA-enriched proteins are known to be membrane proteins. Since membrane proteins generally are more hydrophobic than soluble proteins[42], and StA is likely embedded in the membrane as a lipid anchor[43], it could be that the more hydrophobic tetrazine-modified biotin (**19**) is more likely to react with these proteins. However, for compound **17** which is also more hydrophobic, only ~20-30% of the StA-enriched proteins are membrane proteins (as annotated by UniProt keyword KW-0472[47]). This could be explained by the shorter aliphatic linker between the hydrophilic biotin moiety and the reactive tetrazine moiety, making it more difficult for the tetrazine to reach StA embedded in the membranes. For compound **17**, a completely unique set of StA-enriched proteins were detected that were found with neither **19** nor biotin-PEG4-tetrazine, suggesting there might be an interesting application for this compound after all (Figure S8). It is not known which exact molecular properties of the tetrazine-modified biotins are responsible for the described discrepancies, and this would need to be elucidated by further research.

Previous research has highlighted an important role of protein lipidation in the regulation of a large number of immunological proteins.[8,12,55,56] From the significantly StA-enriched proteins that were detected with **17**, **19** and biotin-PEG4-tetrazine, all proteins with a reported immunological function (as annotated by UniProt keyword KW-0391[47]) are listed in Tables S2, S3, and S4, respectively. In addition, the proteins that are known to be lipidated (as annotated by UniProt keyword KW-0449[47]) or membrane proteins (as annotated by UniProt keyword KW-0472[47]) are marked. Several immunological proteins that have not been reported to be lipidated, or even membrane-bound, were identified using the described pull-down method. Most notably is SLC15A3, a transmembrane amino acid transporter located in endolysosomal membranes, that has not before been reported to be lipidated. Several recent reports have highlighted the important role of SLC15A3 in modulating anti-viral innate immune responses, among others in a TLR4-mediated inflammatory response[50], or by inducing type I and type III interferon responses via STING-mediated signalling pathways[57]. SLC15A3 has also been implicated in the escape of bacterially derived components from the endolysosomal system to the cytosol, which in turn activates the NOD2 signalling pathway.[51] SLC15A3 was also found to be upregulated in mature DCs (Figure 5C), again implicating its importance in modulating immune responses. Considering the powerful regulatory role protein lipidation can have, the oleoylation of SLC15A3 could therefore be a novel regulatory mechanism of this important immunomodulatory protein. However, the exact mechanism behind this regulation is not known, and further research is necessary to shine light on this complex interplay.

Conclusion

Here, it has been shown that proteins can be modified with StA as a PTM. This was confirmed by labelling StA-modified proteins with a fluorophore and resolving the proteins by SDS-PAGE, as well as labelling the proteins with tetrazine-modified biotins and performing pull-down chemical proteomics. A library of tetrazine-modified biotins was synthesised and assessed for their cell-permeability, as well as reactivity with StA. Two compounds (**17** and **19**) showed sufficient permeability and reactivity and were used in a live-cell click pull-down proteomics approach. This approach was compared to a click-on-lysate approach with biotin-PEG4-tetrazine. It appears that both the timing of the IEDDA reaction, and the physicochemical properties of the tetrazine-modified biotins affect which lipidated proteins are detected. The current research could not fully elucidate the underlying mechanisms of these discrepancies, and further research is needed to understand this. Several proteins with known immunological functions, that have never been reported to be lipidated, were also identified. The important innate immunoregulatory protein SLC15A3 was shown to be lipidated for the first time, indicating that this could be a regulatory mechanism for its activation.

Acknowledgements

Maxime Legierse and Dr. Ward Doelman are acknowledged for their synthesis of the tetrazine-modified biotin library. Dr. Bogdan I. Florea and Dr. Berend Gagestein are acknowledged for their help with acquiring, processing, and analysing the LC-MS/MS data. Prof. Kenneth L. Rock is thanked for his kind gift of the DC2.4 cell line.

Materials & Methods

Chemical synthesis

General

All reactions were performed using dried glassware and reagent grade solvents. All commercially available reagents used were obtained via Sigma-Aldrich and Merck and were used as received. Anhydrous solvents were prepared by keeping activated 4 Å molecular sieves in the solvents for at least 24 h. Flash chromatography was performed silica gel 60 (0.04-0.063 mm). TLC analysis was conducted on Merck aluminum sheets and silica gel 60 F254 sheets. TLC analyses were visualized using 254 nm UV absorption and by using ninhydrin staining followed by charring at ~150 ℃. ^{1}H and ^{13}C NMR spectra were recorded using the Bruker AV Liquid 400 MHz and Bruker AV WB 400 MHz spectrometer. Samples were measured in $CDCl_3$, MeOD DMSO-D_6 or D_2O. Chemical shifts (δ) are reported in ppm compared to either trimethyl silane (0 ppm) or the solvent residual peak as internal standard. Coupling constants are reported in Hz. Assigning individual signals of the final compounds was aided by HH-COSY.

9: tert-butyl (4-cyanobenzyl) carbamate

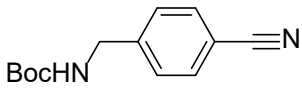

Di-tert-butyldicarbonate (22 mmol, 4.80 g, 1.1 eq) and NaOH (60 mmol, 2.40 g, 3 eq) were added to 40 mL H_2O. (4-aminomethyl)-benzonitrile (20 mmol, 3.37 g) was added and the reaction was stirred overnight at RT. The precipitate was filtered and concentrated under reduced pressure to yield compound **9** as a white solid (4.11 g, 17.7 mmol, 89%).

^{1}H NMR (400 MHz, $CDCl_3$) δ 7.61 (d, *J* = 8.3 Hz, 2H, $CH_{aromatic}$), 7.38 (d, *J*= 8.3 Hz, 2H, $CH_{aromatic}$), 5.03 (s, 1H, NH), 4.36 (d, *J* = 6.3 Hz, 2H, CH_2), 1.45 (s, 9H, $CH_{3\ Boc}$). **^{13}C NMR** (101 MHz, $CDCl_3$) δ 146.8 ($C_{q\ aromatic}$), 144.7 ($C_{q\ boc\ carbonyl}$), 132.5 ($CH_{aromatic}$), 127.9 ($CH_{aromatic}$), 118.9 ($C_{q\ nitrile}$), 111.2 ($C_{q\ aromatic}$), 80.1 ($C_{q\ tbu}$), 44.3 (CH_2), 28.4-27.5 ($CH_{3\ Boc}$)

22: tert-butyl (2-cyanoethyl) carbamate

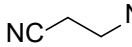

3-Amino propionitrile (10 mmol, 0.70 g) and Boc_2O (12 mmol, 2.76 mL, 1.2 eq.) were added to 20 mL anhydrous DCM. The reaction was stirred overnight at RT. The organic layer was washed with water and brine, dried over $MgSO_4$ and filtered. The organic layer was concentrated under reduced pressure to yield compound **22** as a clear oil (1.67 g, 9.8 mmol, 98%).

^{1}H NMR (400 MHz, $CDCl_3$) δ 5.05 (s, 1H, NH), 3.40 (q, *J* = 6.3 Hz, 2H, CH_2), 2.60 (t, *J* = 6.3 Hz, 2H, CH_2), 1.45 (d, *J* = 1.6 Hz, 9H, $CH_{3\ Boc}$). **^{13}C NMR** (101 MHz, $CDCl_3$) δ 118.3 ($C_{q\ nitrile}$), 80.3 ($C_{q\ tBu}$), 36.9 (CH_2), 28.4-27.5 ($CH_{3\ Boc}$), 19.1 (CH_2).

General tetrazine synthesis (10-12 and 23-25)

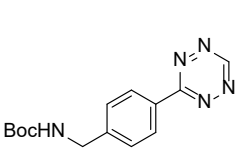

10.

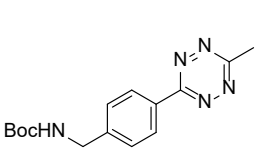

11.

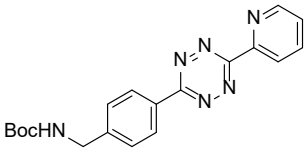

12.

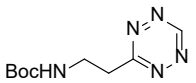

23.

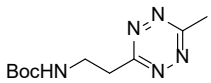

24.

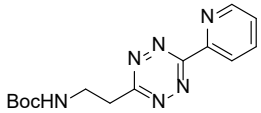

25.

The N-Boc protected carbonitrile (compound **9** or **22**; 1 eq.) was added to a pressure tube. To this tube a Lewis acid catalyst ($Zn(OTf)_2$ or $Ni(OTf)_2$; 0.25 eq.), the corresponding carbonitrile (acetonitrile, formamidine acetate or 2-cyanopyridine; 5 eq.) and 64% hydrazine monohydrate (50 eq.) were added. If required, dry dioxane (1.6 mL/mmol) was added as an additional solvent and the pressure tube was sealed. The reaction mixture was heated and stirred overnight. After cooling down to RT the rubber seal was carefully punctured to release the NH_3 gas. For oxidation of the dihydrotetrazines, two different procedures were used as described below. After oxidation, column purification yielded tetrazines **10**-**12** and **23**-**25** as pink solids.

Procedure A: The suspension was slowly added to a mixture of AcOH/DCM (1:1, v:v, 20 mL/mmol). Next, $NaNO_2$ (20 eq.) was added over a period of 30 minutes. When gas formation ceased, the mixture was concentrated under reduced pressure, and the resulting mass was redissolved in EtOAc. The organic layer was washed three times with H_2O and three times with $NaHCO_3$ (sat.) and subsequently dried over $MgSO_4$, filtered, and concentrated in vacuo.

Procedure B: The suspension was added to an aqueous 4M $NaNO_2$ solution (80 eq., 20 mL/mmol). Next, aqueous 2M HCl (120 eq., 60 mL/mmol) was added dropwise until gas formation had ceased. The mixture was further diluted with aqueous 0.1M HCl (50 mL/mmol) was added, and the product was extracted three times with EtOAc (50 mL/mmol). The organic layer was dried over $MgSO_4$, filtered and concentrated under reduced pressure.

10: tert-butyl (4-(1,2,4,5-tetrazin-3-yl)benzyl)carbamate

Compound **9** (5 mmol, 1.16 g), $Zn(OTf)_2$ (1.25 mmol, 0.455 g, 0.25 eq) formamidine acetate (50 mmol, 5.20 g, 10 eq) and 64% hydrazine monohydrate (250 mmol, 12.1 mL, 50 eq) were used. The reaction was stirred overnight at 60°C. Oxidation procedure A was performed and column purification (1% -> 5%, EtOAc in DCM) yielded **10** as a pink solid (128 mg, 0.4 mmol, 9%).

^{1}H NMR (400 MHz, $CDCl_3$) δ 10.22 (s, 1H, tetrazine-H), 8.60 (d, *J* = 8.1 Hz, 2H, $CH_{aromatic}$), 7.53 (d, *J* = 8.1 Hz, 2H, $CH_{aromatic}$), 4.98 (s, 1H, NH), 4.46 (d, *J* = 6.2 Hz, 2H, CH_2), 1.48 (s, 9H, $CH_{3\ Boc}$). **^{13}C NMR** (101 MHz, $CDCl_3$) δ 166.4 ($C_{q\ tetrazine}$), 161.3 ($C_{q\ Boc\ carbonyl}$), 157.9 ($CH_{tetrazine}$), 144.8 ($C_{q\ aromatic}$), 130.7 ($C_{q\ aromatic}$), 128.7 ($CH_{aromatic}$),

128.3 ($CH_{aromatic}$), 44.5 (CH_2), 28.5 ($CH_{3\ Boc}$).

11: tert-butyl (4-(6-methyl-1,2,4,5-tetrazin-3-yl)benzyl)carbamate

Compound **9** (2 mmol, 0.464 g) was dissolved in acetonitrile (10 mmol, 0.522 mL, 5 eq) in a pressure tube. $Zn(OTf)_2$ (0.5 mmol, 0.182 g, 0.25 eq) and 64% hydrazine monohydrate (100 mmol, 4.84 mL, 50 eq) were added and the reaction was stirred overnight at 80°C. Oxidation procedure A was performed and column purification (2% -> 10%, EtOAc in DCM) yielded **11** as a pink solid (197 mg, 0.7 mmol, 33%).

^{1}H NMR (400 MHz, $CDCl_3$) δ 8.51 (d, *J* = 8.4 Hz, 2H, $CH_{aromatic}$), 7.48 (d, *J* = 8.4 Hz, 2H, $CH_{aromatic}$), 5.21 (s, 1H, NH), 4.43 (d, *J* = 6.1 Hz, 2H, CH_2), 3.09 (s, 3H, CH_3), 1.48 (s, 9H, $CH_{3\ Boc}$). **^{13}C NMR** (101 MHz, $CDCl_3$) δ 167.2 ($C_{q\ tetrazine}$), 163.9 ($C_{q\ tetrazine}$), 156.1 ($C_{q\ Boc\ carbonyl}$), 144.1 ($C_{q\ aromatic}$), 130.8 ($C_{q\ aromatic}$), 128.2 ($CH_{aromatic}$), 128.1 ($CH_{aromatic}$), 79.8 ($C_{q\ Boc\ tBu}$), 44.4 (CH_2), 28.5 ($CH_{3\ Boc}$), 21.2 (CH_3).

12: tert-butyl (4-(6-(pyridin-2-yl)-1,2,4,5-tetrazin-3-yl)benzyl)carbamate

Compound **9** (2 mmol, 0.464 g) was dissolved in 2-cyanopyridine (10 mmol, 0.962 mL, 5eq) in a pressure tube. $Zn(OTf)_2$ (0.5 mmol, 0.182 g, 0.25 eq) and 64% hydrazine monohydrate (100 mmol, 4.84 mL, 50 eq) were added and the reaction was stirred overnight at 80°C. Oxidation procedure A was performed and column purification (2% -> 20%, EtOAc in DCM) yielded **12** as a pink solid (213 mg, 0.6 mmol, 29%).

^{1}H NMR (400 MHz, $CDCl_3$) δ 8.97 (d, *J* = 0.9 Hz, 1H, CH_{pyr}), 8.69 (d, *J* = 1.1 Hz, 1H, CH_{pyr}), 8.65 (d, 2H, $CH_{aromatic}$), 8.00 (td, *J* = 7.8, 1.8 Hz, 1H, $CH_{aromatic}$), 7.57 (dd, *J* = 4.8, 1.2 Hz, 1H, CH_{pyr}), 7.54 (d, *J* = 8.2 Hz, 2H, $CH_{aromatic}$), 5.12 (s, 1H, NH), 4.46 (d, *J* = 6.1 Hz, 2H, CH_2), 1.49 (s, 9H, $CH_{3\ Boc}$). **^{13}C NMR** (101 MHz, $CDCl_3$) δ 164.3 ($C_{q\ tetrazine}$), 163.5 ($C_{q\ tetrazine}$), 156.1 ($C_{q\ Boc\ carbonyl}$), 151.0 (CH_{pyr}), 150.4 ($C_{q\ pyr}$), 144.7 ($C_{q\ aromatic}$), 137.6 (CH_{pyr}), 130.6 ($C_{q\ aromatic}$), 128.8 ($CH_{aromatic}$), 128.2 ($CH_{aromatic}$), 126.5 (CH_{pyr}), 124.0 (CH_{pyr}), 80.4 ($C_{q\ Boc\ tBu}$), 44.5 (CH_2), 28.5 ($CH_{3\ Boc}$).

23: tert-butyl (2-(1,2,4,5-tetrazin-3-yl)ethyl)carbamate

Compound **22** (1 mmol, 0.170 g), formamidine acetate (5 mmol, 0.521 g, 5 eq.), $Zn(OTf)_2$ (0.25 mmol, 0.090 g, 0.25 eq.) and dry dioxane (1.5 mL) were added to a pressure tube. 64% Hydrazine monohydrate (50 mmol. 2.42 mL, 50 eq.) was added dropwise and the reaction was stirred for 3 days at RT. Oxidation procedure B was performed, and column purification (5% EtOAc in DCM) yielded product **23** as a pink oil (6 mg, 0.02 mmol, 2%).

^{1}H NMR (400 MHz, $CDCl_3$) δ 10.24 (s, 1H, tetrazine-H), 5.01 (s, 1H, NH), 3.84 – 3.72 (m, 2H, CH_2), 3.57 (dd, *J* = 6.9, 5.4 Hz, 2H, CH_2), 1.38 (s, 9H, $CH_{3\ Boc}$).

24: tert-butyl (2-(6-methyl-1,2,4,5-tetrazin-3-yl)ethyl)carbamate

Compound **22** (1.65 mmol, 0.280 g), acetonitrile (19 mmol, 1 mL, 11 eq.), nickel triflate (0.25 mmol, 0.090 g, 0.15 eq.) and dry dioxane (2.6 mL) were added to a

pressure tube. 64% hydrazine monohydrate (76 mmol, 2.4 mL, 50 eq.) was added dropwise and the reaction was stirred overnight at 60°C. Oxidation procedure A was performed with 13 equivalents of $NaNO_2$. Column purification (3% → 10% EtOAc in DCM) yielded product **24** as a pink oil (7 mg, 0.03 mmol, 3%).

^{1}H NMR (400 MHz, $CDCl_3$) δ 5.02 (s, 1H, NH), 3.74 (td, *J* = 6.6, 5.5 Hz, 2H, CH_2), 3.51 (t, *J* = 6.2 Hz, 2H, CH_2), 3.06 (s, 3H, CH_3), 1.38 (s, 9H, $CH_{3\ Boc}$). **^{13}C NMR** (101 MHz, $CDCl_3$) δ 67.2 ($C_{q\ tBu}$), 38.4 (CH_2), 35.5 (CH_2), 28.4 (CH_3), 21.2 ($CH_{3\ Boc}$).

25: tert-butyl (2-(6-(pyridin-2-yl)-1,2,4,5-tetrazin-3-yl)ethyl)carbamate

Compound **22** (1 mmol, 0.17 g), 2-cyanopyridine (5 mmol, 0.49 mL, 5 eq.) and zinc triflate (0.25 mmol, 0.09 g, 0.25 eq.) were added to nitrogen flushed flask. Hydrazine monohydrate (50 mmol, 2.5 g, 50 eq.) was added and the mixture was stirred overnight at 60°C under nitrogen atmosphere. Oxidation procedure B was performed and column purification (30% → 65% EtOAc in pentane) yielded product **25** as a pink oil (68 mg, 0.2 mmol, 22%).

^{1}H NMR (400 MHz, $CDCl_3$) δ 8.96 (d, *J* = 4.7 Hz, 1H, CH_{pyr}), 8.65 (d, *J* = 8.0 Hz, 1H, CH_{pyr}), 7.99 (td, *J* = 7.8, 1.9 Hz, 1H, CH_{pyr}), 7.57 (t, *J* = 6.3 Hz, 1H, CH_{pyr}), 4.34 (dt, *J* = 7.9, 3.9 Hz, 2H, CH_2), 3.56 – 3.47 (m, 2H, CH_2), 1.25 (s, 9H, $CH_{3,\ Boc}$). **^{13}C NMR** (101 MHz, $CDCl_3$) δ 151.4 (CH_{pyr}), 137.9 (CH_{pyr}), 127.0 (CH_{pyr}), 124.5 (CH_{pyr}), 86.4 ($C_{q\ Boc}$), 33.1 (CH_2), 30.2 (CH_2), 28.4 ($CH_{3,\ Boc}$).

General Boc-deprotection (13-15 and 26-28)

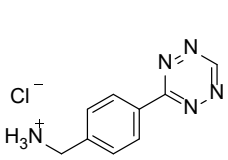
13.

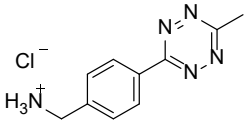
14.

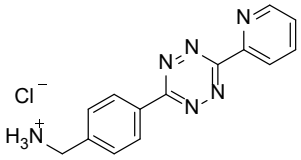
15.

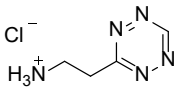
26.

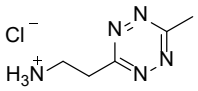
27.

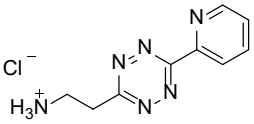
28.

The Boc-protected tetrazine was dissolved in dry DCM (1 mL/30 mg) and 4M HCl in dioxane (1 mL / 30 mg) was added to the reaction mixture dropwise. The reaction was stirred for 2h at RT under N_2 atmosphere. The suspension was centrifuged, and the supernatant was removed. The pellet was washed two times via resuspension in 10 mL dry dioxane. The pellet was then resuspended in 5 mL dry dioxane and concentrated under reduced pressure yielding compounds **13**-**15** and **26**-**28** as colored N-Boc deprotected ammonium chloride salts. ^{1}H NMRs of synthesized compounds were consistent with previously reported NMR results of these compounds. Low concentrations and the instability of compounds **13**-**14** and **26**-**28** caused not all ^{13}C NMRs to be recorded.

13: (4-(1,2,4,5-tetrazin-3-yl)phenyl)methanamonium chloride

Compound **10** (0.1 mmol, 0.027 g) was used and resulted in the N-Boc deprotected product **13** as a pink hydrochloride salt (12 mg, 0.06 mmol, 55%).

^{1}H NMR (400 MHz, MeOD) δ 10.39 (s, 1H, tetrazine-H), 8.68 (d, *J* = 8.6 Hz, 2H, $CH_{aromatic}$), 7.75 (d, *J* = 0.6 Hz, 2H, $CH_{aromatic}$), 4.28 (s, 2H, CH_2). **^{13}C NMR** (101 MHz, MeOD) δ 168.4 ($C_{q\ tetrazine}$), 167.7 ($CH_{tetrazine}$), 157.4 ($C_{q\ aromatic}$), 143.0 ($C_{q\ aromatic}$), 130.9 ($CH_{aromatic}$), 129.8 ($CH_{aromatic}$), 43.9 (CH_2).

14: (4-(6-methyl-1,2,4,5-tetrazin-3-yl)phenyl)methanamonium chloride

Compound **11** (0.1 mmol, 0.03 g) was used and resulted in the N-Boc deprotected product **14** as a pink hydrochloride salt (21 mg, 0.09 mmol, 87%).

^{1}H NMR (400 MHz, MeOD) δ 8.62 (d, *J* = 8.5 Hz, 2H, $CH_{aromatic}$), 7.74 (d, *J* = 8.4 Hz, 2H, $CH_{aromatic}$), 4.28 (s, 1H, NH), 3.05 (s, 3H, CH_3).

15: (4-(6-(pyridin-2-yl)-1,2,4,5-tetrazin-3-yl)phenyl)methanamonium chloride

Compound **12** (0.082 mmol, 0.03 g) was used and resulted in the N-Boc deprotected product **15** as a purple hydrochloride salt (24 mg, 0.08 mmol, 96%).

^{1}H NMR (400 MHz, MeOD) δ 9.16 (d, *J* = 8.1 Hz, 1H, CH_{pyr}), 9.08 (d, *J* = 4.6 Hz, 1H, CH_{pyr}), 8.80 (d, *J* = 8.4 Hz, 2H, $CH_{aromatic}$), 8.76 (dd, *J* = 8.0, 1.6 Hz, 1H, CH_{pyr}), 8.27 – 8.22 (m, 1H, CH_{pyr}), 7.82 (d, *J* = 8.6 Hz, 2H, $CH_{aromatic}$), 4.32 (s, 2H, CH_2). **^{13}C NMR** (101 MHz, MeOD) δ 165.9 ($C_{q\ tetrazine}$), 161.7 ($C_{q\ tetrazine}$), 147.0 - 146.8 (m, CH_{pyr}, $C_{q\ pyr}$), 140.1 ($C_{q\ aromatic}$), 133.5 ($C_{q\ aromatic}$), 131.2 ($CH_{aromatic}$), 130.4 (CH_{pyr}), 126.9 (CH_{pyr}), 43.9 (CH_2).

26: (4-(1,2,4,5-tetrazin-3-yl)phenyl)methanamonium chloride

Compound **23** (13 µmol, 3 mg) was used and resulted in the N-Boc deprotected product **26** as a pink hydrochloride salt (2 mg, 0.01 mmol, 93%).

^{1}H NMR (400 MHz, MeOD) δ 10.44 (s, 1H, tetrazine-H), 3.80 – 3.71 (m, 2H, CH_2), 3.67 (d, *J* = 10.4 Hz, 2H, CH_2).

27: 2-(6-methyl-1,2,4,5-tetrazin-3-yl)ethan-1-amonium chloride

Compound **24** (0.031 mmol, 7.3 mg) was used and resulted in the N-Boc deprotected product **27** as a pink hydrochloride salt (7 mg, 0.04 mmol, quant.).

28: 2-(6-(pyridin-2-yl)-1,2,4,5-tetrazin-3-yl)ethan-1-amonium chloride

Compound **25** (0.034 mmol, 0.01 g) was used and resulted in the N-Boc deprotected product **28** as a pink hydrochloride salt (9 mg, 0.04 mmol, quant.).

^{1}H NMR (400 MHz, MeOD) δ 9.13 (d, *J* = 8.1 Hz, 1H, CH_{pyr}), 9.07 (d, *J* = 5.5 Hz, 1H, CH_{pyr}), 8.74 (t, 1H, CH_{pyr}), 8.24 (t, *J* = 6.7 Hz, 1H, CH_{pyr}), 3.92 (t, *J* = 6.9 Hz, 2H, CH_2), 3.73 (t, *J* = 6.9 Hz, 2H, CH_2).

General synthesis biotin-tetrazines (16-21 and 29-31)

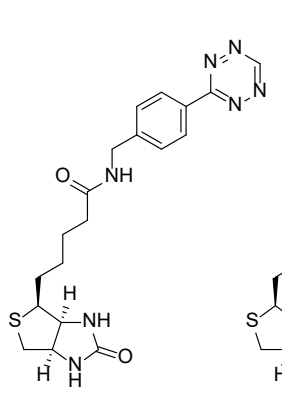

16.

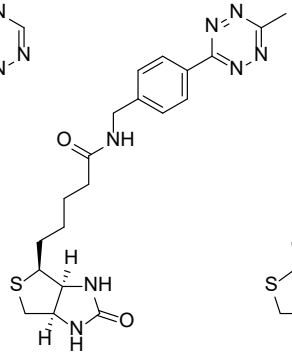

17.

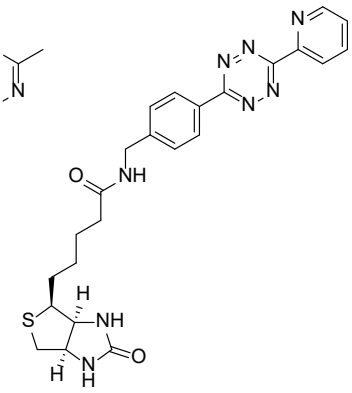

18.

The NHS-biotins were dissolved in DCM after which the tetrazine ammonium salt (1.2 eq.) and DIPEA (2 eq.) were added. The reaction mixture was stirred for 3h at RT for tetrazines **13**-**15** and stirred for 24h at RT for tetrazines **26**-**28**. Completion of the reaction was checked with LC-MS and the mixture was concentrated. After purification by HPLC all fractions containing the product were pooled and lyophilized, which yielded the biotin-tetrazines **16**-**21** and **29**-**31** as pink solids. Final compounds were obtained in small amounts causing ^{13}C NMR signals to be too weak to be measured for some of the compounds.

16: N-(4-(1,2,4,5-tetrazin-3-yl)benzyl)-5-(2-oxohexahydro-1H-thieno[3,4-d]imidazol-4-yl)pentanamide

NHS-biotin (0.046 mmol, 0.016 g) was dissolved in 2.4 mL DCM. Compound **13** (0.055 mmol, 0.012 g, 1.2 eq) and DIPEA (0.092 mmol, 0.016 mL, 2 eq) were added to the reaction mixture. After purification compound **16** was obtained as a pink solid (14.0 mg, 0.03 mmol, 73%).

^{1}H NMR (400 MHz, DMSO-D_6, HH-COSY) δ 10.58 (s, 1H, tetrazine-H), 8.49 (d, *J* = 6.1 Hz, 1H, NH_{amide}), 8.46 (d, *J* = 8.3 Hz, 2H, $CH_{aromatic}$), 7.53 (d, *J* = 8.4 Hz, 2H, $CH_{aromatic}$), 6.44 (s, 1H, NH_{biotin}), 6.36 (s, 1H, NH_{biotin}), 4.39 (d, *J* = 6.0 Hz, 2H, CH_2), 4.33 – 4.27 (m, 1H, CH_{biotin}), 4.17 – 4.09 (m, 1H, CH_{biotin}), 3.14 – 3.07 (m, 1H, CH_{biotin}), 2.82 (dd, *J* = 12.5, 5.1 Hz, 1H, $CH_{2\ biotin}$), 2.57 (d, *J* = 21.2 Hz, 1H, $CH_{2\ biotin}$), 2.19 (t, *J* = 7.4 Hz, 2H, $CH_{2\ linker}$), 1.68 – 1.26 (m, 6H, $CH_{2\ linker}$).

HRMS: calculated for $C_{19}H_{24}N_7O_2S$ [M+H]+ 414.17; found 414.17138

17: N-(4-(6-methyl-1,2,4,5-tetrazin-3-yl)benzyl)-5-(2-oxohexahydro-1H-thieno[3,4-d] imidazol-4-yl) pentanamide

NHS-biotin (0.073 mmol, 0.025 g) was dissolved in 3.75 mL DCM. Compound **14** (0.087 mmol, 0.021 g, 1.2 eq) and DIPEA (0.145 mmol, 0.025 mL, 2 eq) were added to the reaction. After purification compound **17** was obtained as a pink solid. (16.3 mg, 0.04 mmol, 53%).

^{1}H NMR (400 MHz, DMSO-D_6) δ 8.47 (t, *J* = 6.0 Hz, 1H, NH_{amide}), 8.42 (d, *J* = 8.4 Hz, 2H, $CH_{aromatic}$), 7.51 (d, *J* = 8.3 Hz, 2H, $CH_{aromatic}$), 6.44 (s, 1H, NH_{biotin}), 6.36 (s, 1H, NH_{biotin}), 4.38 (d, *J* = 6.0 Hz, 2H, CH_2), 4.30 (dd, 1H, CH_{biotin}), 4.16 – 4.09 (m, 1H, CH_{biotin}), 3.10 (dt, *J* = 8.7, 5.6 Hz, 1H, CH_{biotin}), 2.99 (s, 3H, CH_3), 2.82 (dd, *J* = 12.5, 5.1 Hz, 1H, $CH_{2\ biotin}$), 2.67 (q, *J* = 1.8 Hz, 1H, $CH_{2\ biotin}$), 2.18 (t, *J* = 7.4 Hz, 2H, $CH_{2\ linker}$), 1.67 – 1.29 (m, 6H, $CH_{2\ linker}$). **^{13}C NMR** (101 MHz, DMSO-D_6) δ 175.8 ($C_{q\ carbonyl\ biotin}$), 163.2 ($C_{q\ carbonyl\ amide}$), 148.2 ($C_{q\ tetrazine}$), 144.6 ($C_{q\ tetrazine}$), 134.7 ($C_{q\ aromatic}$), 128.1 ($CH_{aromatic}$), 127.5 ($CH_{aromatic}$), 120.3 ($C_{q\ aromatic}$), 61.1 (CH_{biotin}), 59.2 (CH_{biotin}), 55.5 (CH_{biotin}), 52.0 ($CH_{2\ biotin}$), 41.9 (CH_2), 31.3 ($CH_{2\ linker}$), 25.3 ($CH_{2\ linker}$), 11.6 (CH_3).

HRMS: calculated for $C_{20}H_{26}N_7O_2S$ [M+H]+ 428.19; found 428.18794

18: 5-(2-oxohexahydro-1H-thieno[3,4-d]imidazol-4-yl)-N-(4-(6-(pyridin-2-yl)-1,2,4,5-tetrazin-3-yl)benzyl)pentanamide

NHS-biotin (0.065 mmol, 0.022 g) was dissolved in 3.2 mL DCM. Compound **15** (0.079 mmol, 0.024 g, 1.2 eq) and DIPEA (0.131 mmol, 0.023 mL, 2 eq) were added to the reaction mixture. After purification, compound **18** was obtained as a purple solid. (12.7 mg, 0.03 mmol, 40%).

^{1}H NMR (400 MHz, DMSO-D_6, HH-COSY) δ 8.92 (d, *J* = 4.5 Hz, 1H, CH_{pyr}), 8.57 (d, *J* = 7.9 Hz, 1H, CH_{pyr}), 8.53 (d, *J* = 8.4 Hz, 2H, $CH_{aromatic}$), 8.49 (d, *J* = 6.0 Hz, 1H, NH_{amide}), 8.15 (td, *J* = 7.8, 1.8 Hz, 1H, CH_{pyr}), 7.72 (ddd, *J* = 7.6, 4.7, 1.2 Hz, 1H, CH_{pyr}), 7.56 (d, *J* = 8.4 Hz, 2H, $CH_{aromatic}$), 6.44 (s, 1H, NH_{biotin}), 6.37 (s, 1H, NH_{biotin}), 4.41 (d, *J* = 5.9 Hz, 2H, CH_2), 4.34 – 4.27 (m, 1H, CH_{biotin}), 4.17 – 4.09 (m, 1H, CH_{biotin}), 3.16 – 3.07 (m, 1H, CH_{biotin}), 2.83 (dd, *J* = 12.5, 5.1 Hz, 1H, $CH_{2\ biotin}$), 2.58 (d, *J* = 12.5 Hz, 1H, $CH_{2\ biotin}$), 2.20 (t, *J* = 7.4 Hz, 2H, $CH_{2\ linker}$), 1.66 – 1.31 (m, 6H, $CH_{2\ linker}$). **^{13}C NMR** (101 MHz, DMSO-D_6) δ 172.4 ($C_{q\ carbonyl\ biotin}$), 163.2 ($C_{q\ tetrazine}$), 150.6 (CH_{pyr}), 146.6 ($C_{q\ pyr}$), 145.2 ($C_{q\ aromatic}$), 137.9 (CH_{pyr}), 130.2 ($C_{q\ aromatic}$), 128.2 ($CH_{aromatic}$), 128.0 ($CH_{aromatic}$), 124.0 (CH_{pyr}), 61.1 (CH_{biotin}), 59.3 (CH_{biotin}), 55.5 (CH_{pyr}), 41.9 (CH_2), 33.5 ($CH_{2\ linker}$), 28.1 ($CH_{2\ linker}$), 25.4 ($CH_{2\ linker}$).

HRMS: calculated for $C_{24}H_{27}N_8O_2S$ [M+H]+ 491.20; found 491.19836

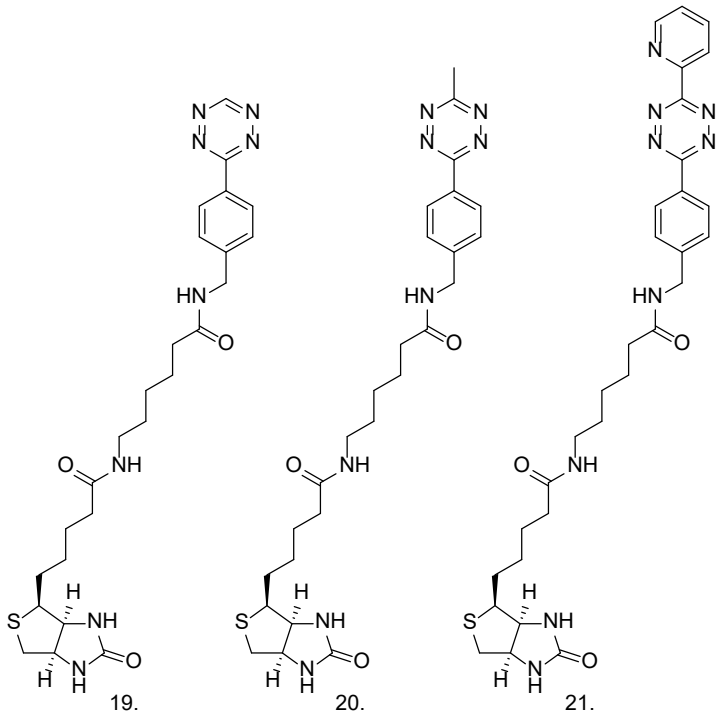

19. 20. 21.

19: N-(4-(1,2,4,5-tetrazin-3-yl)benzyl)-6-(5-(2-oxohexahydro-1H-thieno[3,4-d]imidazol-4-yl)pentanamido)hexanamide

NHS-LC-biotin (0.075 mmol, 0.034 g) was dissolved in 3.75 mL DCM. Compound **13** (0.090 mmol, 0.020 g, 1.2 eq) and DIPEA (0.150 mmol, 0.026 mL, 2 eq) were added to the reaction mixture. After purification, compound **19** was obtained as a pink solid. (23.8 mg, 0.05 mmol, 60%).

^{1}H NMR (400 MHz, DMSO-D_6) δ 10.58 (s, 1H, tetrazine-H), 8.47 (d, *J* = 3.3 Hz, 2H, $CH_{tetrazine}$), 8.45 (t, *J* = 1.9 Hz, 1H, NH_{amide}), 7.76 (t, *J* = 5.6 Hz, 1H, NH_{amide}), 7.53 (d, *J* = 8.3 Hz, 2H, $CH_{tetrazine}$), 6.42 (s, 1H, NH_{biotin}), 6.36 (s, 1H, NH_{biotin}), 4.39 (d, *J* = 6.0 Hz, 2H, CH_2), 4.29 (dd, *J* = 7.8, 4.9 Hz, 1H, CH_{biotin}), 4.12 (dd, *J* = 7.8, 4.4 Hz, 1H, CH_{biotin}), 3.08 (dt, *J* = 8.7, 5.8 Hz, 1H, CH_{biotin}), 3.01 (q, *J* = 6.6 Hz, 2H, $CH_{2\ linker}$), 2.81 (dd, *J* = 12.5, 5.1 Hz, 1H, $CH_{2\ linker}$), 2.58 (s, 1H, CH_2 linker), 2.17 (t, *J* = 7.4 Hz, 2H, $CH_{2\ linker}$), 2.04 (t, *J* = 7.4 Hz, 2H $CH_{2\ linker}$), 1.67 – 1.19 (m, 12H, $CH_{2\ linker}$). **^{13}C NMR** (101 MHz, DMSO-D_6) δ 172.4 ($C_{q\ carbonyl\ amide}$), 171.9 ($C_{q\ carbonyl\ amide}$), 165.5 ($CH_{tetrazine}$), 162.8 ($C_{q\ carbonyl\ biotin}$), 145.1 ($C_{q\ aromatic}$), 130.4 ($C_{q\ aromatic}$), 128.1 ($CH_{aromatic}$), 127.9 ($CH_{aromatic}$), 61.1 (CH_{biotin}), 59.2 (CH_{biotin}), 55.5 (CH_{biotin}), 41.9 (CH_2), 38.4 ($CH_{2\ linker}$), 35.4 ($CH_{2\ linker}$), 35.3 ($CH_{2\ linker}$), 29.0-25.1 ($CH_{2\ linker}$).

HRMS: calculated for $C_{25}H_{35}N_8O_3S$ [M+H]+ 527.26; found 527.25596

20: N-(4-(6-methyl-1,2,4,5-tetrazin-3-yl)benzyl)-6-(5-(2-oxohexahydro-1H-thieno[3,4-d]imidazol-4-yl)pentanamido)hexanamide

NHS-LC-biotin (0.083 mmol, 0.038 g) was dissolved in 4.15 mL DCM. Compound **14** (0.1 mmol, 0.025 g, 1.2 eq) and DIPEA (0.167 mmol, 0.029 mL, 2 eq) were added to the reaction mixture. After purification compound **20** was obtained as a pink solid. (23.2 mg, 0.04 mmol, 52%).

^{1}H NMR (400 MHz, DMSO-D_6) δ 8.46 (d, *J* = 5.9 Hz, 1H, NH_{amide}), 8.42 (d, *J* = 8.3 Hz, 2H, $CH_{aromatic}$), 7.76 (t, *J* = 5.6 Hz, 1H, NH_{amide}), 7.51 (d, *J* = 8.2 Hz, 2H, $CH_{aromatic}$), 6.42 (s, 1H, NH_{biotin}), 6.36 (s, 1H, NH_{biotin}), 4.38 (d, *J* = 6.0 Hz, 2H, CH_2), 4.29 (dd, *J* = 7.7, 4.9 Hz, 1H, CH_{biotin}), 4.12 (dd, *J* = 7.8, 4.4 Hz, 1H, CH_{biotin}), 3.11 – 3.05 (m, 1H, CH_{biotin}), 3.02 (dd, 2H, $CH_{2\ linker}$), 2.99 (s, 3H, CH_3), 2.81 (dd, *J* = 12.5, 5.1 Hz, 1H, $CH_{2\ biotin}$), 2.56 (d, *J* = 12.8 Hz, 1H, $CH_{2\ biotin}$), 2.17 (t, *J* = 7.4 Hz, 2H, $CH_{2\ linker}$), 2.03 (t, *J* = 7.4 Hz, 2H, $CH_{2\ linker}$), 1.59 – 1.20 (m, 12H, $CH_{2\ linker}$). **^{13}C NMR** (101 MHz, DMSO-D_6) δ 172.4 ($C_{q\ carbonyl\ amide}$), 171.9 ($C_{q\ carbonyl\ amide}$), 167.1 ($C_{q\ tetrazine}$), 163.2 ($C_{q\ tetrazine}$), 162.8 ($C_{q\ carbonyl\ biotin}$), 144.6 ($C_{q\ aromatic}$), 130.4 ($C_{q\ aromatic}$), 128.1 ($CH_{aromatic}$), 127.5 ($CH_{aromatic}$), 61.1 (CH_{biotin}), 59.2 (CH_{biotin}), 55.5 (CH_{biotin}), 41.9 (CH_2), 38.4 ($CH_{2\ linker}$), 35.4 ($CH_{2\ linker}$), 35.3 ($CH_{2\ linker}$), 29.0-25.1 ($CH_{2\ linker}$), 20.9 (CH_3).

HRMS: calculated for $C_{26}H_{37}N_8O_3S$ [M+H]+ 541.27; found 541.27139

21: 6-(5-(2-oxohexahydro-1H-thieno[3,4-d]imidazol-4-yl)pentanamido)-N-(4-(6-(pyridin-2-yl)-1,2,4,5-tetrazin-3-yl)benzyl)hexanamide

NHS-LC-biotin (0.062 mmol, 0.028 g) was dissolved in dry DCM (3.1 mL). Compound **15** (0.075 mmol, 0.022 g, 1.2 eq.) and DIPEA (0.124 mmol, 0.022 mL, 2 eq). were added to the reaction mixture. After purification compound **21** was obtained as a purple solid. (15.0 mg, 0.02 mmol, 40%).

^{1}H NMR (400 MHz, DMSO-D_6) δ 8.92 (ddd, *J* = 4.7, 1.8, 0.9 Hz, 1H, CH_{pyr}), 8.57 (dt, *J* = 8.0, 1.1 Hz, 1H, NH_{amide}), 8.56 – 8.51 (m, 2H, $CH_{aromatic}$), 8.48 (t, *J* = 6.0 Hz, 1H, CH_{pyr}), 8.15 (td, *J* = 7.8, 1.8 Hz, 1H, CH_{pyr}), 7.77 (t, *J* = 5.6 Hz, 1H, NH_{amide}), 7.72 (ddd, *J* = 7.6, 4.7, 1.2 Hz, 1H, CH_{pyr}), 7.56 (d, *J* = 8.3 Hz, 2H, $Ch_{aromatic}$), 6.43 (s, 1H, $NH_{amide\ biotin}$), 6.36 (s, 1H, $NH_{amide\ biotin}$), 4.41 (d, *J* = 6.0 Hz, 2H, CH_2), 4.29 (dd, *J* = 7.7, 4.9 Hz, 1H, CH_{biotin}), 4.11 (dd, *J* = 7.8, 4.4 Hz, 1H, CH_{biotin}), 3.12 – 3.05 (m, 1H, CH_{biotin}), 3.01 (q, *J* = 6.6 Hz, 2H, $CH_{2\ linker}$), 2.80 (dd, *J* = 12.4, 5.0 Hz, 1H, $CH_{2\ biotin}$), 2.70 – 2.64 (m, 1H, $CH_{2\ biotin}$), 2.53 (d, *J* = 8.8 Hz, 3H, CH_3), 2.18 (t, *J* = 7.4 Hz, 2H, $CH_{2\ linker}$), 2.04 (t, *J* = 7.4 Hz, 2H, $CH_{2\ linker}$), 1.65 – 1.19 (m, 12H, $CH_{2\ linker}$). **^{13}C NMR** (101 MHz, DMSO-D_6) δ 176.1, 172.5, 171.9, 162.1, 151.6, 150.7, 145.2, 139.7, 130.2, 128.2, 128.0, 61.1, 59.2, 55.5, 41.9, 31.7, 28.1, 26.2, 25.4, 25.1.

HRMS: calculated for $C_{30}H_{38}N_9O_3S$ [M+H]+ 604.28; found 604.28255

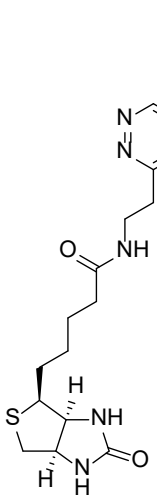
29.

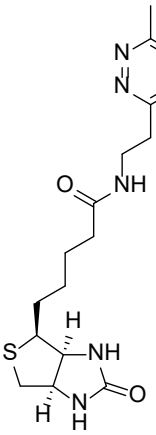
30.

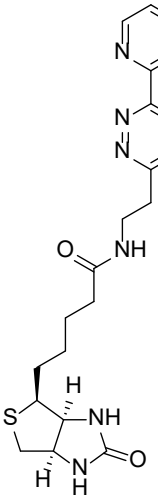
31.

29: N-(2-(1,2,4,5-tetrazin-3-yl)ethyl)-5-(2-oxohexahydro-1H-thieno[3,4-d] imidazol-4-yl)pentanamide

NHS-biotin (0.01 mmol, 3.5 mg) was dissolved in dry DCM (0.7 mL). Compound **26** (0.012 mmol, 2 mg, 1.2 eq.) and DIPEA (0.021 mmol, 3.6 µL, 2 eq.) were added to the reaction mixture. After purification compound **29** was obtained as a pink solid (1.4 mg, 0.004 mmol, 38%).

^{1}H NMR (400 MHz, D_2O, HH-COSY) δ 10.39 (s, 1H, tetrazine-H), 4.59 (t, 1H, CH_{biotin}), 4.41 (t, 1H, CH_{biotin}), 3.77 (t, 2H, CH_2), 3.55 (t, J = 6.3 Hz, 2H, CH_2), 3.33 – 3.22 (m, 1H, CH_{biotin}), 2.98 (dd, 1H, $CH_{2\ biotin}$), 2.76 (d, J = 13.1 Hz, 1H, $CH_{2\ biotin}$), 2.14 (t, J = 7.3 Hz, 2H, $CH_{2\ linker}$), 1.78 – 1.22 (m, 6H, $CH_{2\ linker}$).

HRMS: calculated for $C_{14}H_{22}N_7O_2S$ [M+H]+ 352.16; found 352.15587

30: N-(2-(6-methyl-1,2,4,5-tetrazin-3-yl)ethyl)-5-(2-oxohexahydro-1H-thieno[3,4-d]imidazol-4-yl)pentanamide

NHS-biotin (0.026 mmol, 8.9 mg) was dissolved in dry DCM (1.8 mL). Compound **27** (0.031 mmol, 5.4 mg, 1.2 eq.) and DIPEA (0.052 mmol, 9 µL, 2 eq.) were added to the reaction mixture. After purification, compound **30** was obtained as a pink solid (7.0 mg, 0.02 mmol, 73%).

^{1}H NMR (400 MHz, D_2O) δ 4.59 (dd, *J* = 7.8, 5.2 Hz, 1H, CH_{biotin}), 4.39 (dd, *J* = 8.2, 4.4 Hz, 1H, CH_{biotin}), 3.74 (q, *J* = 5.2 Hz, 2H,CH_2), 3.48 (t, *J* = 6.4 Hz, 2H, CH_2), 3.27 (dt, *J* = 9.5, 5.0 Hz, 1H, CH_{biotin}), 3.02 (d, *J* = 1.7 Hz, 3H, CH_3), 3.00 – 2.93 (m, 1H, $CH_{2\ biotin}$), 2.75 (d, *J* = 13.1 Hz, 1H, $CH_{2\ biotin}$), 2.13 (t, *J* = 7.2 Hz, 2H, $CH_{2\ linker}$), 1.77 – 1.18 (m, 6H, $CH_{2\ linker}$).**^{13}C NMR** (101 MHz, D_2O) δ 167.8, 62.1 (CH_{biotin}), 60.3 (CH_{biotin}), 55.3 (CH_{biotin}), 39.7 (CH_2).

HRMS: calculated for $C_{15}H_{24}N_7O_2S$ [M+H]+ 366.17; found 366.17139

31: 5-(2-oxohexahydro-1H-thieno[3,4-d]imidazol-4-yl)-N-(2-(6-(pyridin-2-yl)-1,2,4,5-tetrazin-3-yl)ethyl)pentanamide

NHS-biotin (0.033 mmol, 0.011 mg) was dissolved in dry DCM (2.2 mL). Compound **28** (0.039 mmol, 9.3 µg, 1.2 eq.) and DIPEA (0.065 mmol, 11 µL, 2 eq.) were added to the reaction mixture. After purification compound **31** was obtained as a pink solid (3.3 mg, 0.01 mmol, 35%).

^{1}H NMR (400 MHz, D_2O) δ 8.70 (s, 1H, CH_{pyr}), 8.52 (d, *J* = 8.0 Hz, 1H, CH_{pyr}), 8.09 (t, *J* = 7.9 Hz, 1H, CH_{pyr}), 7.66 (s, 1H, CH_{pyr}), 4.29 (s, 1H, CH_{biotin}), 4.10 (s, 1H, CH_{biotin}), 3.70 (d, *J* = 16.9 Hz, 2H, CH_2), 3.48 (s, 2H, CH_2), 2.97 (s, 1H, $CH_{2\ biotin}$), 2.77 – 2.59 (m, 1H, $CH_{2\ biotin}$), 2.51 – 2.37 (m, 1H, CH_{biotin}), 1.99 (t, *J* = 6.9 Hz, 2H, $CH_{2\ linker}$), 1.47 – 0.90 (m, 6H, $CH_{2\ linker}$)

HRMS: calculated for $C_{19}H_{25}N_8O_2S$ [M+H]+ 429.18; found 429.18243

Biological experiments

General. Sterculic acid (StA) was purchased from Cayman Chemical (#26735), and stored as 10 mM or 100 mM stock solutions in DMSO at -20°C. The tetrazine-fluorophore conjugates **3** and **7** were synthesised in-house (see Chapter 2 of this thesis), and were stored as 2 mM stock solutions in DMSO at -20°C. Biotin-PEG4-tetrazine was purchased from Conju-Probe (#CP-6001), and stored as an 80 mM stock solution in DMSO at -20°C. The other biotin-tetrazines (**16**-**21** and **29**-**31**) were synthesised in-house as described above, and stored as 10 mM stock solutions in DMSO at -80°C. Streptavidin AZDye 647 (Monovalent) labelling reagent was purchased from Abcam (#ab272190), and stored as delivered at 4°C.

Culturing of DC2.4 cells. DC2.4 cells were cultured in RPMI 1640 culture medium (Gibco, #31870025) supplemented with 10% FCS, GlutaMAX (2 mM), sodium pyruvate (1 mM), 1x non-essential amino acids (NEAA, Thermo Fisher Scientific), penicillin (100 I.U./mL), streptomycin (50 µg/mL), and 2-mercaptoethanol (50 µM, Thermo Fisher Scientific), and incubated at 37°C, 5% CO_2. The cells were grown to 70-80% confluency and passaged every 2-3 days by trypsinisation.

SDS-PAGE analysis of protein lipidation with sterculic acid. $3.4x10^5$ cells were seeded per well in a 6-well plate (Sarstedt) and allowed to attach for 20 h at 37°C, 5% CO_2. Half the samples were stimulated with LPS-EB Ultrapure (100 mg/mL, InvivoGen) in fresh culture medium, while the other half got refreshed culture medium. All dishes were incubated 24 h at 37°C, 5% CO_2, and washed with medium x2. StA (100 µM) or DMSO vehicle (0.1%) in fresh culture medium were added to the dishes and incubated for 20 h at 37°C, 5% CO_2. The click-on-live-cell samples (Figure 2B) were washed with medium x2 before 10 µM of fluorophore **7** in fresh culture medium was added. The cells were incubated for 2 h at 37°C, 5% CO_2. Medium was aspirated and all cells were washed with PBS x2, harvested by scraping in ice-cold PBS, and centrifuged at 1000 *g*, 5 min. Supernatant was aspirated and cell pellets were lysed by resuspension in cold lysis buffer (sucrose

(250 mM) and $MgCl_2$ (1 mM) in PBS supplemented with 1x EDTA-free protease inhibitor (Roche)). Samples were incubated 10 min on ice with occasional vortexing, followed by sonication (Qsonica Q700 Microplate Sonicator, 2 x 10 s pulses, 10% amplitude, 0°C). Protein concentrations were measured by Qubit assay (Invitrogen) according to the manufacturer's protocol, and all samples were adjusted to 1 mg/mL in 10 µL lysis buffer. 5 µL of 3x concentrated click-mix (30 µM fluorophore **3** in PBS) were added to the click-on-lysate (Figure 2A) samples to give a final fluorophore concentration of 10 µM. Samples were incubated in the dark at RT for 2 h, before addition of 5 µL 4x Laemmli buffer (without 2-mercaptoethanol) to all samples and incubation at RT for 20 min to ensure all proteins were completely denatured. The samples were resolved by SDS-PAGE (12.5% acrylamide gel, ±80 min, 175 V) alongside protein marker (PageRuler Plus, Thermo Fisher Scientific) until the bromophenol blue had just come off the gel. In-gel fluorescence was measured in the AlexaFluor 488- Cy3-, and Cy5-channels on a Chemidoc MP imaging system (Bio-Rad), before subsequent staining with Coomassie, followed by destaining and imaging as a loading control.

Microscopy to verify cell-permeability of biotin-Tzs. $7x10^4$ DC2.4 cells were seeded per well in a flat-bottom 96-well plate. The plates were incubated at 37°C, 5% CO_2 overnight to let the cells attach. StA (100 µM) or DMSO vehicle (0.1%) in fresh culture medium were added to the dishes and incubated for 1 h at 37°C, 5% CO_2. All wells were washed with medium x2. For the live-cell click reaction, wells were treated with biotin-tetrazines **16**-**21** and **29**-**31** (200 µM), biotin-PEG4-tetrazine (200 µM) or DMSO vehicle (2%) in medium for 0 h or 4 h at 37°C, 5% CO_2. All live-click samples were washed with medium x3, followed by PBS x3. All wells were fixed with 4% PFA in PBS for 30 min. Samples were stored in 0.5% PFA in PBS for maximum one week at 4°C until further processing. All wells were washed with PBS x1, followed by glycine (20 mM) in PBS x1. The cells were permeabilised with saponin (0.01%) in PBS for 15 min and washed with PBS x2. All wells were blocked with BSA (1%) in PBS for 1 h. For the fixed-cell click reaction, wells were at this point treated with biotin-tetrazines **16**-**21** and **29**-**31** (200 µM), biotin-PEG4-tetrazine (200 µM) or DMSO vehicle (2%) in BSA (1%) in PBS for 0 h or 4 h at 37°C. The fixed-click samples were washed with BSA (1%) in PBS x6, and all wells were stained with streptavidin AZDye 647 (1:3000) at RT for 1 h. All wells were washed with PBS x4, before counterstaining the nuclei with Hoechst 33342 (2 µg/mL) in PBS for 10 min. The wells were washed with PBS x1 and glycerol/DABCO mounting medium was added. The samples were imaged with the 20x objective of an EVOS M7000 Imaging System (Thermo Fisher Scientific), using the DAPI and Cy5 channels.

Chemical proteomics on StA-treated DC2.4 cells. $7.5x10^5$ DC2.4 cells were seeded in 6 cm dishes in triplicate and allowed to attach for 20 h at 37°C, 5% CO_2. Cells were then either treated with LPS-EB Ultrapure (100 ng/mL, InvivoGen) or vehicle (PBS) in fresh medium for 24 h. Cells were then washed with medium twice and StA (10 µM) or vehicle (0.1% DMSO) was added. After 20 h of incubation, the medium was aspirated. Live-cell click samples were washed with fresh medium x2, before adding compound **17** or **19** (200 µM) diluted in fresh medium, and incubating the samples at 37°C, 5% CO_2 for 4 h to allow the compounds to react with StA. After the click reaction, the samples were washed with fresh medium x2 followed by DPBS x2. Simultaneously, the samples to be clicked-in-lysate were washed with DPBS x2, and all samples were harvested by scraping in ice-cold DPBS. Cells were pelleted by

centrifugation (1000 *g*, 5 min), supernatant was aspirated and cell pellets were lysed by resuspension in cold lysis buffer (Sucrose (250 mM) and $MgCl_2$ (1 mM) in PBS with 2x EDTA-free protease inhibitor (Roche)). Cells were lysed by vortexing followed by sonication (Qsonica Q700 Microplate Sonicator, 2x10 s pulses, 10% amplitude, 0°C). Protein concentration was measured by Qubit Protein assay (Invitrogen) and all samples were adjusted to the lowest protein concentration. To assist membrane solubility, 0.1% Triton X-100 was added to the click-on-lysate samples followed by click reaction with biotin-PEG4-tetrazine (200 µM) at 37°C for 4 h. The volume of all samples was adjusted to 520 µL with PBS and proteins were precipitated by addition of MeOH (666 µL), $CHCl_3$ (166 µL) and MilliQ (150 µL), vortexing after each addition. After spinning down (1500 *g*, 10 min) the upper and lower layer were aspirated and the protein pellet was resuspended in MeOH (600 µL) by sonication (Qsonica Q700 Microplate Sonicator, 2 x 10 s pulses, 10% amplitude). The proteins were spun down (20 000 *g*, 5 min) and the supernatant was discarded.

The proteins were redissolved in 500 µL PBS containing 0.5% SDS and 5 mM DTT by heating to 65°C for 15 minutes, allowed to cool to RT and alkylated by addition of IAA (15 µL, 0.5 M) for 30 min. Excess IAA was quenched with DTT (5 µL, 1 M) and samples were transferred to Eppendorf tubes containing 500 µL PBS and 25 µL prewashed Pierce™ High Capacity Streptavidin Agarose slurry (Thermo Fisher Scientific). Samples were agitated (1000 rpm) for 2 h to ensure binding to the beads, which were then spun down (3.000 *g*, 2 min). Supernatant was discarded and beads were washed with PBS containing 0.5% SDS (3X) and PBS (3X). Beads were resuspended in MilliQ, transferred to Protein LoBind tubes (Eppendorf), spun down (3000 *g*, 2 min) and supernatant was discarded. The beads were resuspended in digestion buffer (200 µL, 100 mM Tris pH 7.8, 100 mM NaCl, 1 mM $CaCl_2$, 2% (v/v) acetonitrile, sequencing-grade trypsin (Promega, 0.25 µg)) and incubated while shaking overnight (16 h, 37°C, 1000 rpm). Beads were spun down (3000 *g*, 2 min) and supernatant containing tryptic peptides were transferred to new Protein LoBind tubes. The beads were washed with a 10% formic acid solution (100 µL), which was transferred to the previously isolated peptides. Peptides were desalted using C18 StageTips preconditioned with 50 µL MeOH, 50 µL of 0.5% (v/v) FA in 80% (v/v) acetonitrile/MilliQ (solution B) and 50 µL 0.5% (v/v) FA in MilliQ (solution A) by centrifugation (600 *g*, 2 min). The peptides were washed with solution A (100 µL, 800 *g*, 3 min) and eluted into new Protein LoBind tubes using solution B (100 µL, 800 *g*, 3 min). Samples were concentrated using an Eppendorf SpeedVac (Eppendorf Concentrator Plus 5301 or 5305) and stored at -80°C until measurement.

Nano-LC-MS settings for pull-down samples. Desalted peptide samples were reconstituted in 25-35 µL LC-MS solution (97:3:0.1 H_2O, ACN, FA) containing 10 fmol/µL yeast enolase digest (cat. 186002325, Waters) as injection control. Injection amount was titrated using a pooled quality control sample to prevent overloading the nanoLC system and the automatic gain control (AGC) of the QExactive mass spectrometer. The desalted peptides were separated on a UltiMate 3000 RSLCnano system set in a trap-elute configuration with a nanoEase M/Z Symmetry C18 100 Å, 5 µm, 180 µm x 20 mm (Waters) trap column for peptide loading/retention and nanoEase M/Z HSS C18 T3 100 Å, 1.8 µm, 75 µm x 250 mm (Waters) analytical column for peptide separation. The column was kept at 40°C in a column oven. Samples were injected on the trap column at a flow rate of 15 µL/min for 2 min with 99% mobile phase A (0.1% FA in ULC-MS grade water (Biosolve)), 1% mobile

phase B (0.1% FA in ULC-MS grade acetonitrile (Biosolve)) eluent. The 85 min LC method, using mobile phase A and mobile phase B controlled by a flow sensor at 0.3 µL/min with average pressure of 400-500 bar (5500-7000 psi), was programmed as gradient with linear increment to 1% B from 0 to 2 min, 5% B at 5 min, 22% B at 55 min, 40% B at 64 min, 90% B at 65 to 74 min and 1% B at 75 to 85 min. The eluent was introduced by electro-spray ionization (ESI) via the nanoESI source (Thermo Fisher Scientific) using stainless steel Nano-bore emitters (40 mm, OD 1/32", ES542, Thermo Fisher Scientific).

The QExactive HF was operated in positive mode with data dependent acquisition without the use of lock mass, default charge of 2+ and external calibration with LTQ Velos ESI positive ion calibration solution (88323, Pierce, Thermo Fisher Scientific) every 5 days to less than 2 ppm. The tune file for the survey scan was set to scan range of 350 – 1400 m/z, 120,000 resolution (m/z 200), 1 microscan, automatic gain control (AGC) of 3e6, max injection time of 100 ms, no sheath, aux or sweep gas, spray voltage ranging from 1.7 to 3.0 kV, capillary temp of 250°C and an S-lens value of 80. For the 10 data dependent MS/MS events the loop count was set to 10 and the general settings were resolution to 15,000, AGC target 1e5, max IT time 50 ms, isolation window of 1.6 m/z, fixed first mass of 120 m/z and normalized collision energy (NCE) of 28 eV. For individual peaks the data dependent settings were 1.00e3 for the minimum AGC target yielding an intensity threshold of 2.0e4 that needs to be reached prior of triggering an MS/MS event. No apex trigger was used, unassigned, +1 and charges >+8 were excluded with peptide match mode preferred, isotope exclusion on and dynamic exclusion of 10 sec.

In between experiments, routine wash and control runs were done by injecting 5 µl LC-MS solution containing 5 µL of 10 fmol/µL BSA or enolase digest and 1 µL of 10 fmol/µL angiotensin III (Fluka, Thermo)/oxytocin (Merck) to check the performance of the platform on each component (nano-LC, the mass spectrometer (mass calibration/ quality of ion selection and fragmentation) and the search engine).

Data processing of pull-down samples. Raw files were analysed with MaxQuant (Version 2.0.1.0). The following changes were made to the standard settings of MaxQuant: Label-free quantification (LFQ) was chosen with an LFQ minimal ratio count of 1. Match between runs and iBAQ quantification was enabled. Searches were performed against a Uniprot database of the *Mus Musculus* proteome (UPID: UP000000589, downloaded April 13th, 2022) including the internal standard (yeast enolase P00924). The "proteinGroups.txt" file was used for further analysis in Microsoft Excel, and R Statistical Software[58] (Version 4.3.0). StA-enriched proteins were selected by filtering the proteins for detection by 2+ unique peptides, not found in the reverse decoy FASTA file. At most 1 missing LFQ value in the positive samples (+StA) was allowed, and missing values were imputed with the average value of the two remaining measurements. In cases where three values were missing from the negative samples (DMSO vehicle), the missing values were imputed with a negligible small number to allow for further processing and statistical calculations. Significantly StA-enriched proteins were determined using the empirical Bayes method in the Limma package[59] (Version 3.58.1) in R, and these proteins were determined to have a 2-fold difference between average LFQ values between StA- or vehicle-treated samples with an adjusted p-value of <0.05.

Supplementary Figures & Tables

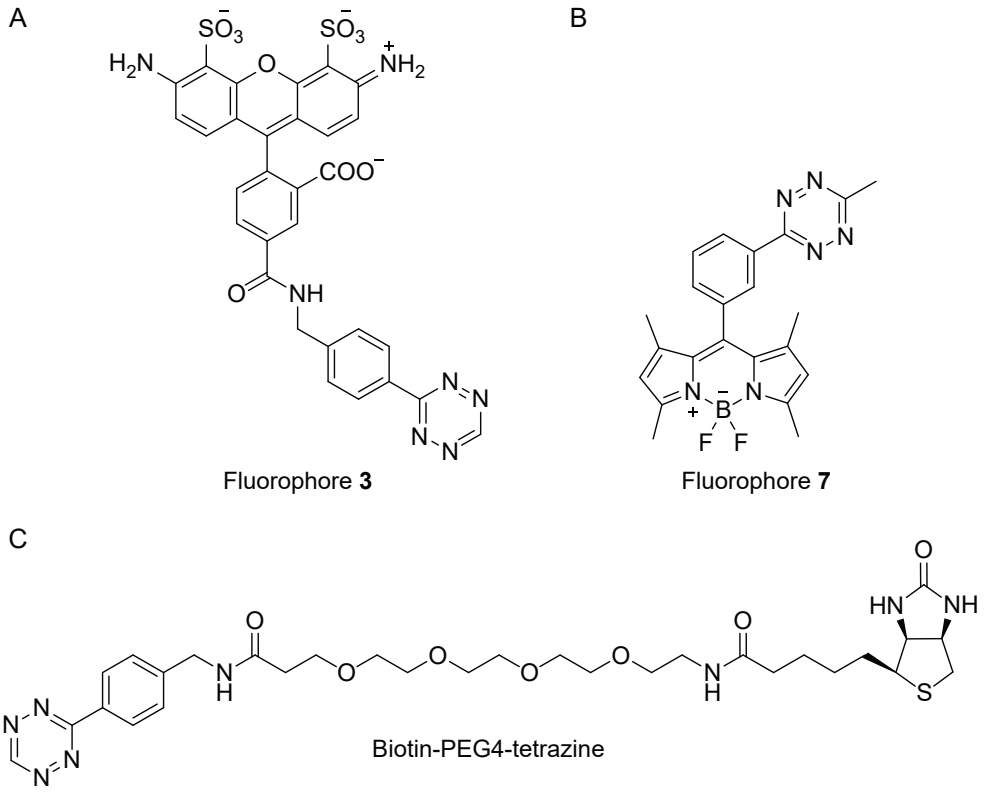

Figure S1: *Structures of* ***A)*** *fluorophore* ***3*** *from Chapter 2,* ***B)*** *fluorophore* ***7*** *from Chapter 2,* ***C)*** *biotin-PEG4-tetrazine.*

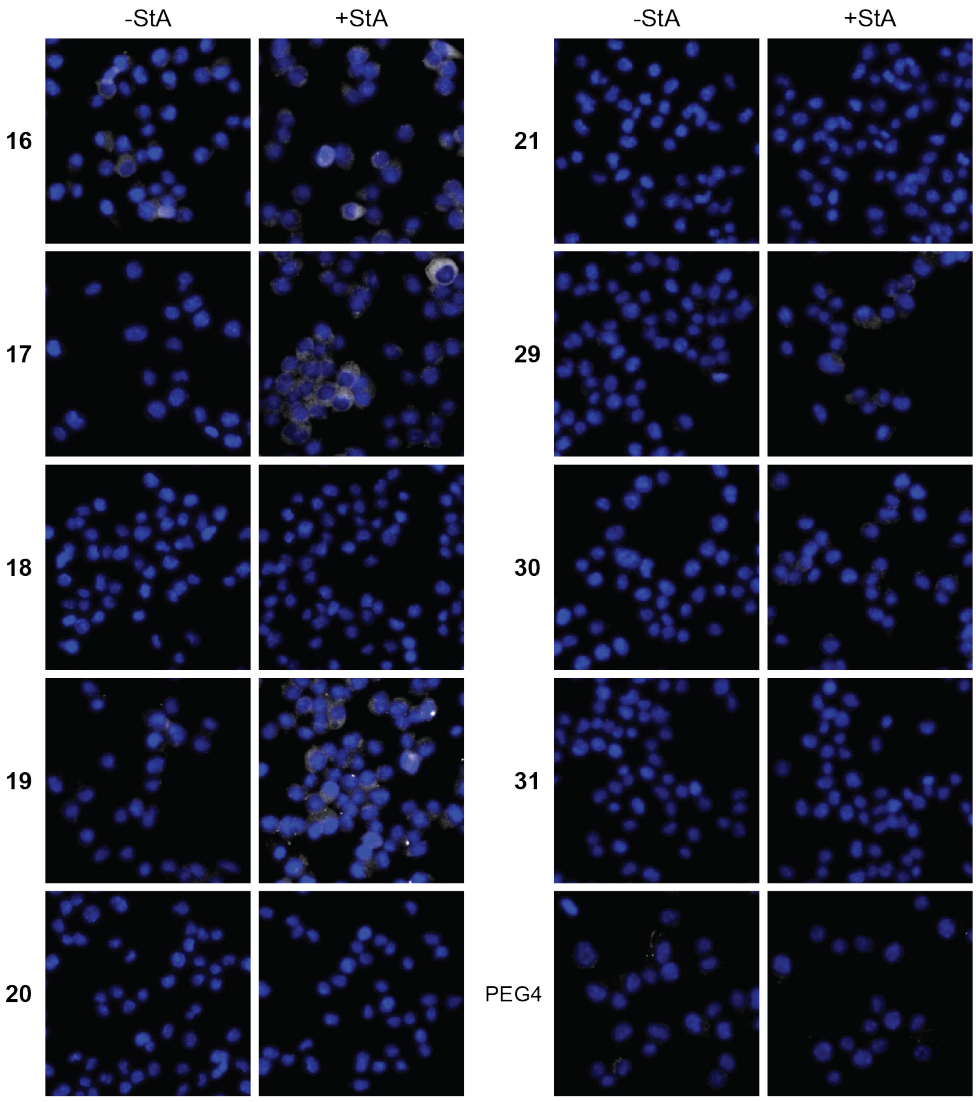

Figure S2: *Fluorescent microscopy to verify cell-permeability of tetrazine-modified biotins* ***16-21****,* ***29-31****, and biotin-PEG4-tetrazine in live DC2.4 cells. To allow uptake of the fatty acid, the cells were incubated with sterculic acid (+StA, 100 µM) or vehicle control (-StA) for 1 h. Then the respective tetrazine-modified biotins (200 µM) were added and incubated for 4 h, before unreacted compound was washed away. The cells were fixed and permeabilised, and a streptavidin AZDye 647 conjugate (grey) was added to visualise the location of the reacted biotins. The nuclei were counterstained with Hoechst 33342 (blue) for reference.*

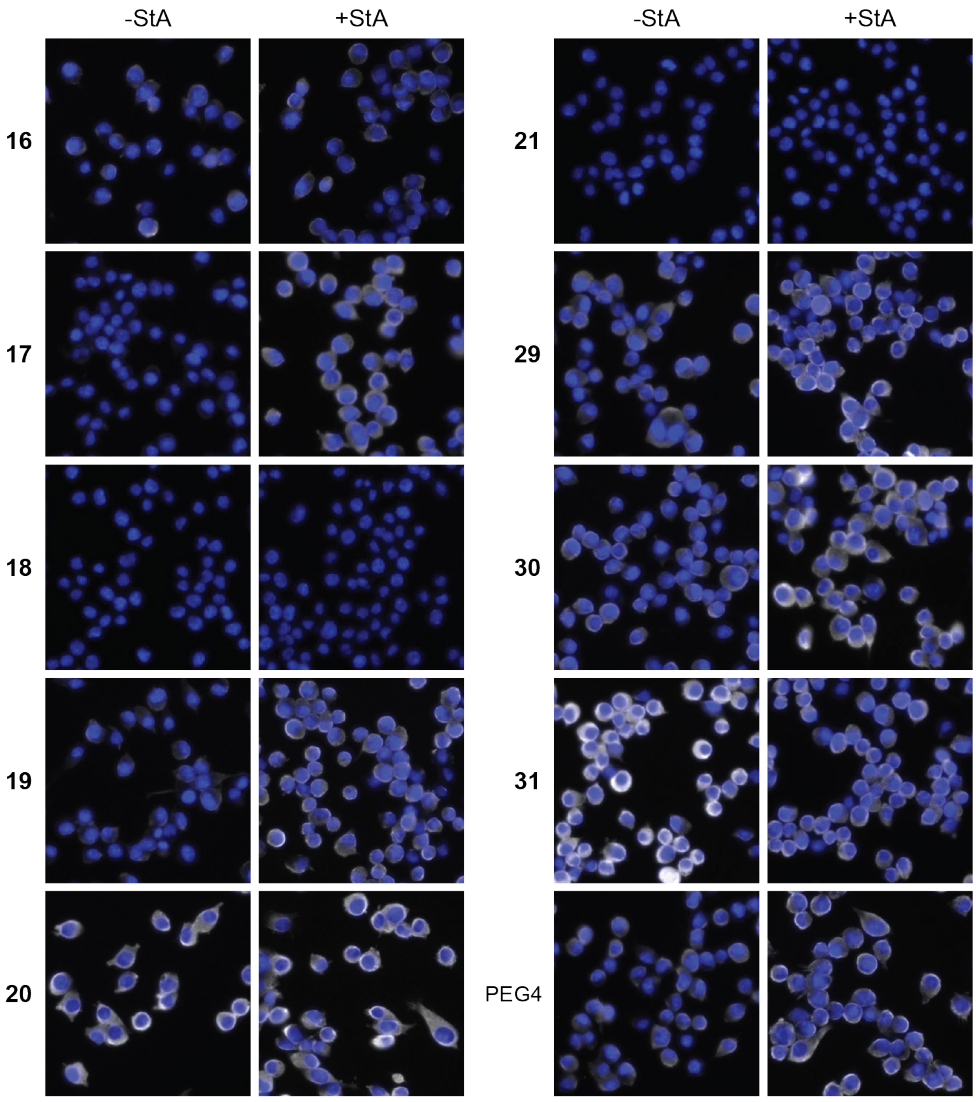

Figure S3: *Fluorescent microscopy to verify reactivity to sterculic acid (StA) of tetrazine-modified biotins* ***16***-***21***, ***29***-***31****, and biotin-PEG4-tetrazine in fixed DC2.4 cells. To allow uptake of the fatty acid, the cells were incubated with StA (+StA, 100 µM) or vehicle control (-StA) for 1 h. The cells were fixed and permeabilised before the respective tetrazine-modified biotins (200 µM) were added and incubated for 4 h. Unreacted compound was washed away, and a streptavidin AZDye 647 conjugate (grey) was added to visualise the location of the reacted biotins. The nuclei were counterstained with Hoechst 33342 (blue) for reference.*

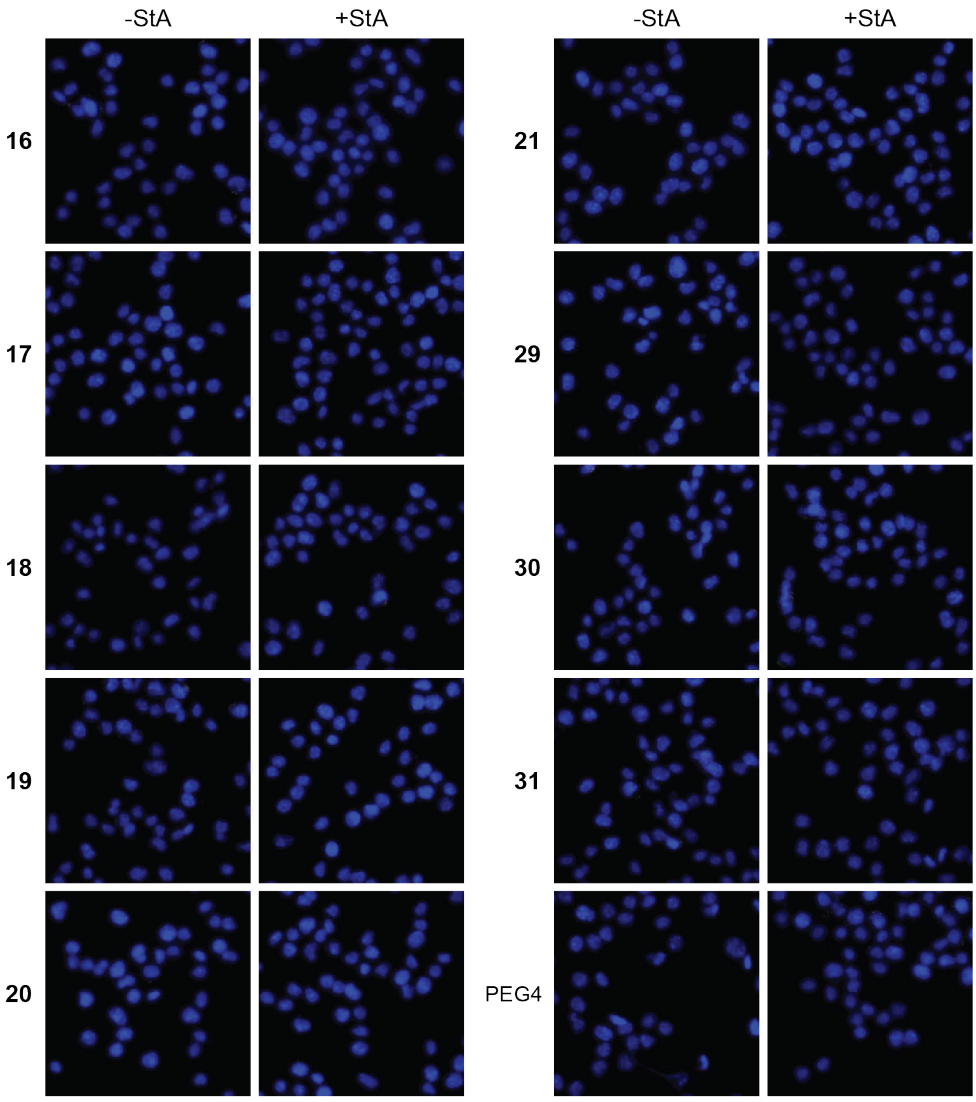

Figure S4: *Control fluorescent microscopy to ensure there is no background fluorescence when the tetrazine-modified biotins* ***16****-****21****,* ***29****-****31****, and biotin-PEG4-tetrazine are not added to live DC2.4 cells. To allow uptake of the fatty acid, the cells were incubated with sterculic acid (+StA, 100 µM) or vehicle control (-StA) for 1 h. Then vehicle control (for the tetrazine-modified biotins) was added and incubated for 4 h. The cells were fixed and permeabilised, and a streptavidin AZDye 647 conjugate (grey) was added to visualise the background fluorescence. The nuclei were counterstained with Hoechst 33342 (blue) for reference.*

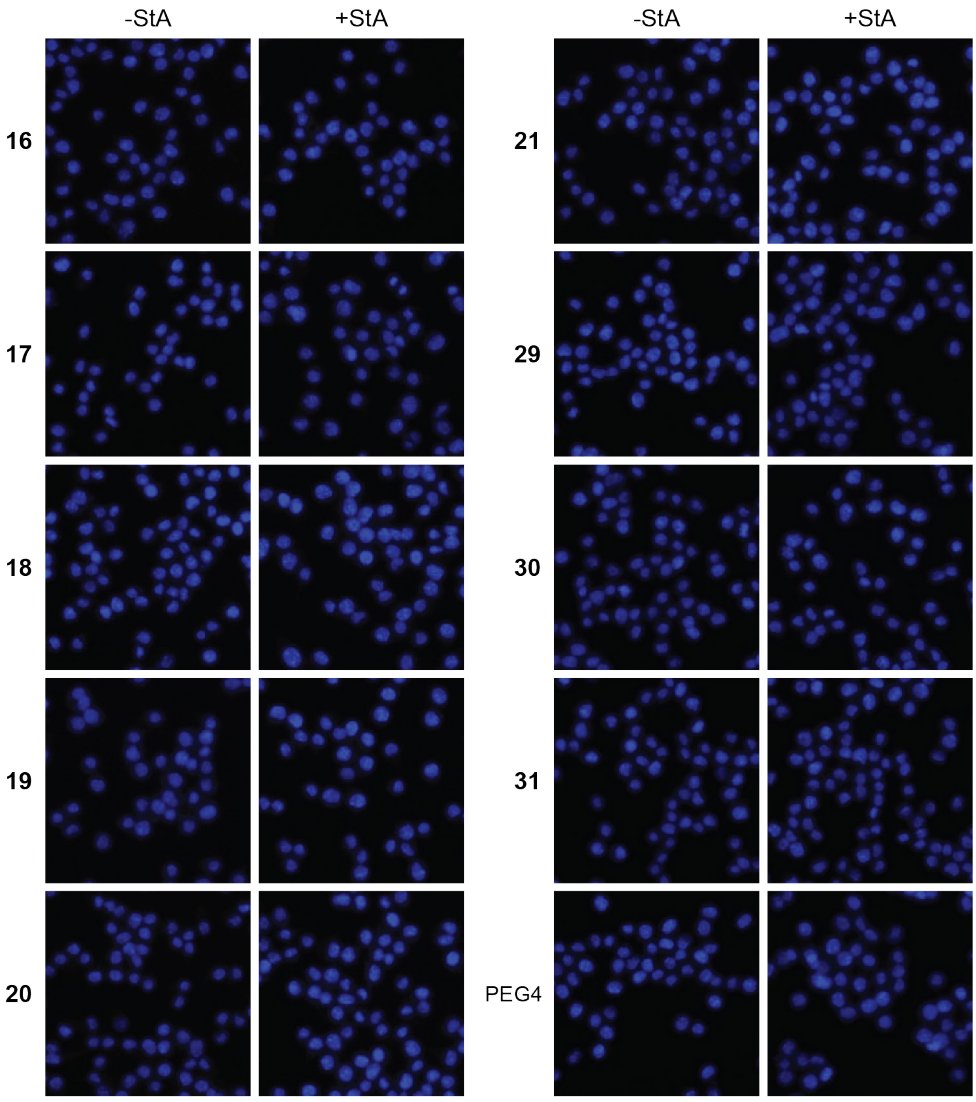

Figure S5: *Control fluorescent microscopy to ensure there is no background fluorescence when the tetrazine-modified biotins* ***16****-****21****,* ***29****-****31****, and biotin-PEG4-tetrazine are not added to fixed DC2.4 cells. To allow uptake of the fatty acid, the cells were incubated with sterculic acid (+StA, 100 µM) or vehicle control (-StA) for 1 h. The cells were fixed and permeabilised, and the vehicle control (for the tetrazine-modified biotins) was added and incubated for 4 h. A streptavidin AZDye 647 conjugate (grey) was added to visualise the background fluorescence. The nuclei were counterstained with Hoechst 33342 (blue) for reference.*

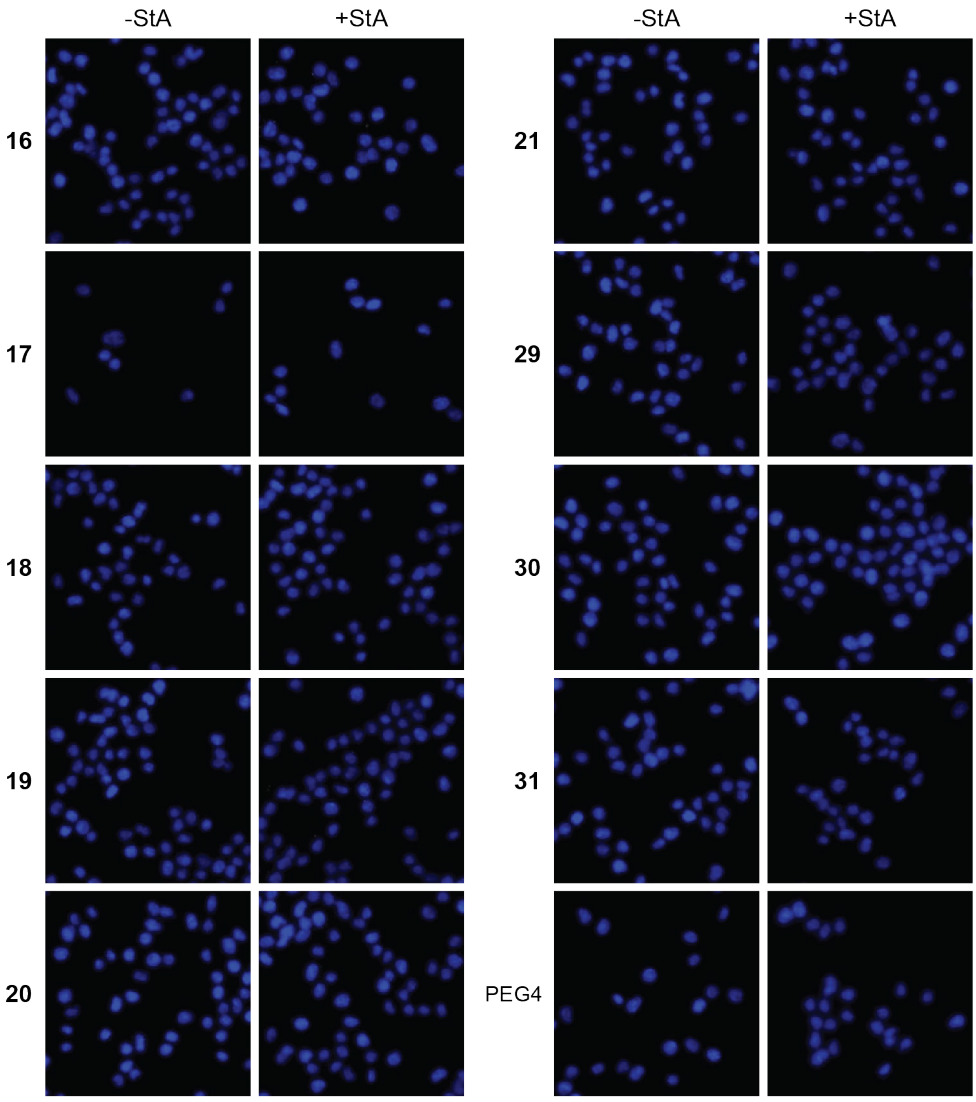

Figure S6: *Control fluorescent microscopy to ensure there is no background fluorescence when the tetrazine-modified biotins* ***16-21***, ***29-31***, *and biotin-PEG4-tetrazine are added to live DC2.4 cells but immediately washed away. To allow uptake of the fatty acid, the cells were incubated with sterculic acid (+StA, 100 µM) or vehicle control (-StA) for 1 h. Then vehicle control (for the tetrazine-modified biotins) was added and incubated for 4 h. The cells were fixed and permeabilised, and a streptavidin AZDye 647 conjugate (grey) was added to visualise the background fluorescence. The nuclei were counterstained with Hoechst 33342 (blue) for reference.*

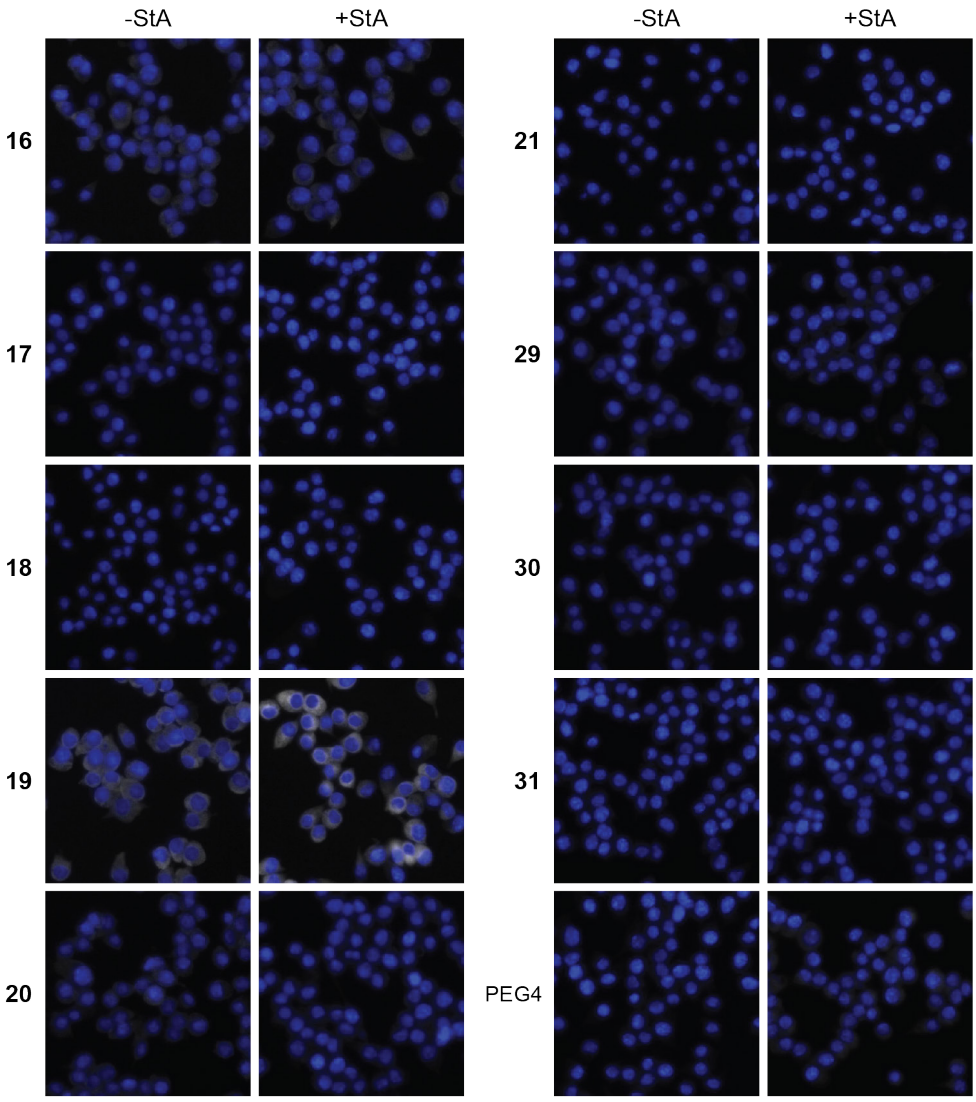

Figure S7: *Control fluorescent microscopy to ensure there is no background fluorescence when the tetrazine-modified biotins* ***16-21****,* ***29-31****, and biotin-PEG4-tetrazine are added to fixed DC2.4 cells but immediately washed away. To allow uptake of the fatty acid, the cells were incubated with sterculic acid (+StA, 100 µM) or vehicle control (-StA) for 1 h. The cells were fixed and permeabilised, and the vehicle control (for the tetrazine-modified biotins) was added and incubated for 4 h. A streptavidin AZDye 647 conjugate (grey) was added to visualise the background fluorescence. The nuclei were counterstained with Hoechst 33342 (blue) for reference.*

Table S1: *List of gene names of the proteins that were found to be significantly enriched with sterculic acid (StA) in immature or mature DC2.4 cells, using compounds* ***17*** *or* ***19****. The proteins that were also found to be significantly StA-enriched with biotin-PEG4-tetrazine are underlined.*

Compound **17** in immature DC2.4s	Compound **17** in mature DC2.4s	Compound **19** in immature DC2.4s	Compound **19** in mature DC2.4s
Fbxo4	*Fbxo4*	*Gk*	*Gk*
Dbnl	*Rpl26*	*Tpcn1*	*Tpcn1*
Lilrb4	*Kif15*	*Vdac2*	*Vdac2*
Tp53bp1	*Fam129b*	*Apc2*	*Plscr1*
Hnrnpd	*Mocos*	*Ptprj*	*Rab5c*
Ppp2r2a/b/d	*Morc3*	*Myo1g*	*Myo1c*
	Gcat	*Ckap4*	*Cds2*
	Rars2	*Slc23a2*	*Tbl3*
	Rps13	*Rpl5*	*Tmem38b*
	Srsf4/6	*Mmd2*	*Rdh11*
		Lbr	*Syk*
			Rcc2
			Npm1
			Pigu
			Mtap
			Sfxn1
			Atp1a1

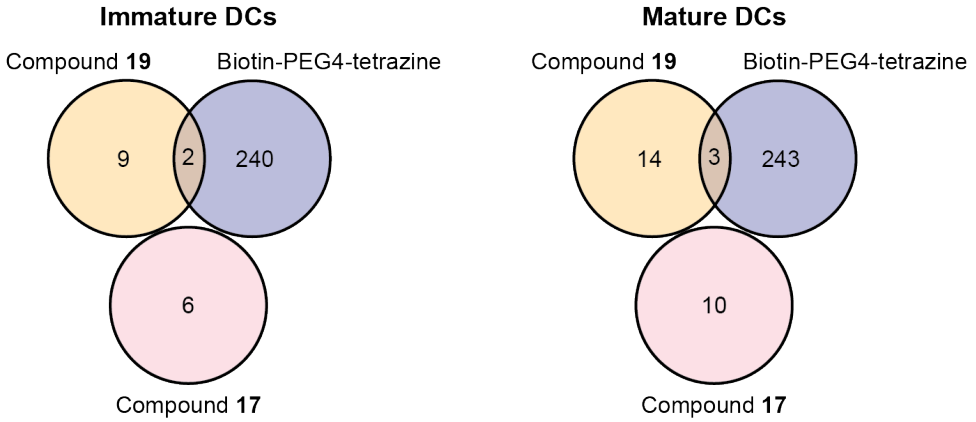

Figure S8: *Venn diagrams showing overlap in proteins that were found to be sterculic acid-enriched with compounds* ***17****,* ***19****, or biotin-PEG4-tetrazine in immature and mature DC2.4 cells.*

Table S2: *Significantly sterculic acid-enriched proteins with known immunological functions (as annotated by UniProt keyword KW-0391[47]), that were detected by compound* ***17*** *in immature or mature DC2.4 cells. Whether the proteins are known to be lipidated (as annotated by UniProt keyword KW-0449[47]) or membrane proteins (as annotated by UniProt keyword KW-0472[47]), is also indicated (with x).*

Immature			**Mature**		
	Lipidated	Membrane		Lipidated	Membrane
Dbnl		x	*Morc3*		
Lilrb4		x			

Table S3: *Significantly sterculic acid-enriched proteins with known immunological functions (as annotated by UniProt keyword KW-0391[47]), that were detected by compound* ***19*** *in immature or mature DC2.4 cells. Whether the proteins are known to be lipidated (as annotated by UniProt keyword KW-0449[47]) or membrane proteins (as annotated by UniProt keyword KW-0472[47]), is also indicated (with x).*

Immature			**Mature**		
	Lipidated	Membrane		Lipidated	Membrane
Myo1g		x	*Syk*		x

Table S4: *Significantly sterculic acid-enriched proteins with known immunological functions (as annotated by UniProt keyword KW-0391[47]), that were detected by biotin-PEG4-tetrazine in immature or mature DC2.4 cells. Whether the proteins are known to be lipidated (as annotated by UniProt keyword KW-0449[47]) or membrane proteins (as annotated by UniProt keyword KW-0472[47]), is also indicated (with x).*

Immature			**Mature**		
	Lipidated	Membrane		Lipidated	Membrane
Cd14	x	x	*Cd14*	x	x
Smpdl3b	x	x	*Smpdl3b*	x	x
Bst2	x	x	*Bst2*	x	x
Mavs	x	x	*Mavs*	x	x
Lat2	x	x	*Lat2*	x	x
Slc15a3		x	*Slc15a3*		x
Mcoln2		x	*Mcoln2*		x
Ctnnbl1			*Ctnnbl1*		
Bag6			*Bag6*		
Ppp6c			*Irak4*		
			Polr3c		

References

1. Ambrogelly, A., Palioura, S. & Söll, D. Natural expansion of the genetic code. *Nature Chemical Biology* **3**, 29–35 (2007).
2. Suazo, K. F., Park, K.-Y. & Distefano, M. D. A Not-So-Ancient Grease History: Click Chemistry and Protein Lipid Modifications. *Chem Rev* **121**, 7178–7248 (2021).
3. Resh, M. D. Fatty acylation of proteins: The long and the short of it. *Prog Lipid Res* **63**, 120–131 (2016).
4. Mann, R. K. & Beachy, P. A. Cholesterol modification of proteins. *Biochimica et Biophysica Acta (BBA) - Molecular and Cell Biology of Lipids* **1529**, 188–202 (2000).
5. Wang, M. & Casey, P. J. Protein prenylation: unique fats make their mark on biology. *Nature Reviews Molecular Cell Biology* **17**, 110–122 (2016).
6. Kinoshita, T. Biosynthesis and biology of mammalian GPI-anchored proteins. *Open Biology* **10**, 190290 (2020).
7. Yuan, Y. *et al.* Protein lipidation in health and disease: molecular basis, physiological function and pathological implication. *Signal Transduction and Targeted Therapy* **9**, 60 (2024).
8. Zhang, Y., Qin, Z., Sun, W., Chu, F. & Zhou, F. Function of Protein S-Palmitoylation in Immunity and Immune-Related Diseases. *Frontiers in Immunology* **12**, (2021).
9. Chesarino, N. M. *et al.* Chemoproteomics reveals Toll-like receptor fatty acylation. *BMC Biology* **12**, 91 (2014).
10. Kim, Y.-C. *et al.* Toll-like receptor mediated inflammation requires FASN-dependent MYD88 palmitoylation. *Nature Chemical Biology* **15**, 907–916 (2019).
11. Mukai, K. *et al.* Activation of STING requires palmitoylation at the Golgi. *Nature Communications* **7**, 11932 (2016).
12. Das, T., Yount, J. S. & Hang, H. C. Protein S-palmitoylation in immunity. *Open Biology* **11**, 200411 (2021).
13. Crise, B. & Rose, J. K. Identification of palmitoylation sites on CD4, the human immunodeficiency virus receptor. *Journal of Biological Chemistry* **267**, 13593–13597 (1992).
14. Balamuth, F., Brogdon, J. L. & Bottomly, K. CD4 Raft Association and Signaling Regulate Molecular Clustering at the Immunological Synapse Site1. *The Journal of Immunology* **172**, 5887–5892 (2004).
15. Arcaro, A. *et al.* Essential Role of CD8 Palmitoylation in CD8 Coreceptor Function1. *The Journal of Immunology* **165**, 2068–2076 (2000).
16. Kabouridis, P. S., Magee, A. I. & Ley, S. C. S-acylation of LCK protein tyrosine kinase is essential for its signalling function in T lymphocytes. *The EMBO Journal* **16**, 4983–4998 (1997).
17. Yurchak, L. K. & Sefton, B. M. Palmitoylation of Either Cys-3 or Cys-5 Is Required for the Biological Activity of the Lck Tyrosine Protein Kinase. *Molecular and Cellular Biology* **15**, 6914–6922 (1995).
18. Kosugi, A. *et al.* A pivotal role of cysteine 3 of Lck tyrosine kinase for localization to glycolipid-enriched microdomains and T cell activation. *Immunology Letters* **76**, 133–138 (2001).
19. Flores, J., White, B. M., Brea, R. J., Baskin, J. M. & Devaraj, N. K. Lipids: chemical tools for their synthesis, modification, and analysis. *Chem Soc Rev* **49**, 4602–4614 (2020).

20. Jao, C. Y., Roth, M., Welti, R. & Salic, A. Metabolic labeling and direct imaging of choline phospholipids in vivo. *Proceedings of the National Academy of Sciences* **106**, 15332–15337 (2009).

21. Jao, C. Y., Roth, M., Welti, R. & Salic, A. Biosynthetic Labeling and Two-Color Imaging of Phospholipids in Cells. *ChemBioChem* **16**, 472–476 (2015).

22. Martin, B. R. & Cravatt, B. F. Large-scale profiling of protein palmitoylation in mammalian cells. *Nature Methods* **6**, 135–138 (2009).

23. Charron, G. *et al.* Robust Fluorescent Detection of Protein Fatty-Acylation with Chemical Reporters. *J Am Chem Soc* **131**, 4967–4975 (2009).

24. Yap, M. C. *et al.* Rapid and selective detection of fatty acylated proteins using ω-alkynyl-fatty acids and click chemistry. *Journal of Lipid Research* **51**, 1566–1580 (2010).

25. Thinon, E. *et al.* Global profiling of co- and post-translationally N-myristoylated proteomes in human cells. *Nat Commun* **5**, 4919 (2014).

26. Wright, M. H. *et al.* Global Analysis of Protein N-Myristoylation and Exploration of N-Myristoyltransferase as a Drug Target in the Neglected Human Pathogen Leishmania donovani. *Chemistry & Biology* **22**, 342–354 (2015).

27. Boyle, P. C. *et al.* Detecting N-myristoylation and S-acylation of host and pathogen proteins in plants using click chemistry. *Plant Methods* **12**, 38 (2016).

28. Storck, E. M. *et al.* Dual chemical probes enable quantitative system-wide analysis of protein prenylation and prenylation dynamics. *Nature Chemistry* **11**, 552–561 (2019).

29. Kallemeijn, W. W. *et al.* Proteome-wide analysis of protein lipidation using chemical probes: in-gel fluorescence visualization, identification and quantification of N-myristoylation, N- and S-acylation, O-cholesterylation, S-farnesylation and S-geranylgeranylation. *Nature Protocols* **16**, 5083–5122 (2021).

30. Hang, H. C. *et al.* Chemical Probes for the Rapid Detection of Fatty-Acylated Proteins in Mammalian Cells. *J Am Chem Soc* **129**, 2744–2745 (2007).

31. Martin, D. D. O. *et al.* Rapid detection, discovery, and identification of post-translationally myristoylated proteins during apoptosis using a bio-orthogonal azidomyristate analog. *The FASEB Journal* **22**, 797–806 (2008).

32. Kostiuk, M. A. *et al.* Identification of palmitoylated mitochondrial proteins using a bio-orthogonal azido-palmitate analogue. *The FASEB Journal* **22**, 721–732 (2008).

33. Witten, A. J. *et al.* Fluorescent imaging of protein myristoylation during cellular differentiation and development. *Journal of Lipid Research* **58**, 2061–2070 (2017).

34. Greaves, J. *et al.* Molecular basis of fatty acid selectivity in the zDHHC family of S-acyltransferases revealed by click chemistry. *Proceedings of the National Academy of Sciences* **114**, E1365–E1374 (2017).

35. Wilson, J. P., Raghavan, A. S., Yang, Y.-Y., Charron, G. & Hang, H. C. Proteomic Analysis of Fatty-acylated Proteins in Mammalian Cells with Chemical Reporters Reveals S-Acylation of Histone H3 Variants. *Molecular & Cellular Proteomics* **10**, M110.001198 (2011).

36. Yount, J. S. *et al.* Palmitoylome profiling reveals S-palmitoylation–dependent antiviral activity of IFITM3. *Nature Chemical Biology* **6**, 610–614 (2010).

37. Cui L, Liu M, Lai S, Hou H, Diao T, Zhang D, Wang M, Zhang Y, W. J. Androgen upregulates the palmitoylation of eIF3L in human prostate LNCaP cells. *Onco Targets Ther.* **12**, 4451–4459 (2019).

38. Sobocińska, J., Roszczenko-Jasińska, P., Ciesielska, A. & Kwiatkowska, K. Protein

Palmitoylation and Its Role in Bacterial and Viral Infections. *Frontiers in Immunology* **8**, (2018).

39. Thinon, E., Percher, A. & Hang, H. C. Bioorthogonal Chemical Reporters for Monitoring Unsaturated Fatty-Acylated Proteins. *ChemBioChem* **17**, 1800–1803 (2016).
40. Montigny, C. *et al.* S-Palmitoylation and S-Oleoylation of Rabbit and Pig Sarcolipin. *Journal of Biological Chemistry* **289**, 33850–33861 (2014).
41. Nůsková, H. *et al.* Stearic acid blunts growth-factor signaling via oleoylation of GNAI proteins. *Nature Communications* **12**, 4590 (2021).
42. Schwartz, R. & King, J. Frequencies of hydrophobic and hydrophilic runs and alternations in proteins of known structure. *Protein Science* **15**, 102–112 (2006).
43. Ray, A., Jatana, N. & Thukral, L. Lipidated proteins: Spotlight on protein-membrane binding interfaces. *Progress in Biophysics and Molecular Biology* **128**, 74–84 (2017).
44. Bertheussen, K. *et al.* Live-Cell Imaging of Sterculic Acid—a Naturally Occurring 1,2-Cyclopropene Fatty Acid—by Bioorthogonal Reaction with Turn-On Tetrazine-Fluorophore Conjugates. *Angewandte Chemie International Edition* **61**, (2022).
45. Devaraj, N. K., Hilderbrand, S., Upadhyay, R., Mazitschek, R. & Weissleder, R. Bioorthogonal Turn-On Probes for Imaging Small Molecules inside Living Cells. *Angewandte Chemie International Edition* **49**, 2869–2872 (2010).
46. Sarris, A. J. C. *et al.* Fast and pH-Independent Elimination of trans-Cyclooctene by Using Aminoethyl-Functionalized Tetrazines. *Chemistry – A European Journal* **24**, 18075–18081 (2018).
47. UniProt: the Universal Protein Knowledgebase in 2023. *Nucleic Acids Research* **51**, 523–531 (2023).
48. Landmann, R. *et al.* Human monocyte CD14 is upregulated by lipopolysaccharide. *Infection and Immunity* **64**, 1762–1769 (1996).
49. Mahnke, K. *et al.* CD14 is Expressed by Subsets of Murine Dendritic Cells and Upregulated by Lipopolysaccharide BT - Dendritic Cells in Fundamental and Clinical Immunology: Volume 3. in (ed. Ricciardi-Castagnoli, P.) 145–159 (Springer US, Boston, MA, 1997). doi:10.1007/978-1-4757-9966-8_25.
50. Song, F. *et al.* Regulation and biological role of the peptide/histidine transporter SLC15A3 in Toll-like receptor-mediated inflammatory responses in macrophage. *Cell Death & Disease* **9**, 770 (2018).
51. Nakamura, N. *et al.* Endosomes are specialized platforms for bacterial sensing and NOD2 signalling. *Nature* **509**, 240–244 (2014).
52. Wang, Y. *et al.* Expression and Regulation of the Proton-Coupled Oligopeptide Transporter PhT2 by LPS in Macrophages and Mouse Spleen. *Molecular Pharmaceutics* **11**, 1880–1888 (2014).
53. Condamine, T. *et al.* Tmem176B and Tmem176A are associated with the immature state of dendritic cells. *Journal of Leukocyte Biology* **88**, 507–515 (2010).
54. Louvet, C. *et al.* Identification of a New Member of the CD20/FcεRIβ Family Overexpressed in Tolerated Allografts. *American Journal of Transplantation* **5**, 2143–2153 (2005).
55. Lin, H. Protein cysteine palmitoylation in immunity and inflammation. *The FEBS Journal* **288**, 7043–7059 (2021).
56. West, S. J., Boehning, D. & Akimzhanov, A. M. Regulation of T cell function by protein S-acylation. *Frontiers in Physiology* **13**, (2022).
57. He, L. *et al.* The Solute Carrier Transporter SLC15A3 Participates in Antiviral

Innate Immune Responses against Herpes Simplex Virus-1. *Journal of Immunology Research* **2018**, 5214187 (2018).

58. R Core Team. R: A Language and Environment for Statistical Computing. Preprint at (2023).
59. Ritchie, M. E. *et al.* limma powers differential expression analyses for RNA-sequencing and microarray studies. *Nucleic acids research* **43**, (2015).
60. Perez-Riverol, Y. *et al.* The PRIDE database resources in 2022: a hub for mass spectrometry-based proteomics evidences. *Nucleic acids research* **50**, 543–552 (2022).